The influence of aerosols on precipitating systems: Analysis of results from the WRF-SBM

Barry H. Lynn[1,2] and Alexander Khain[2]

[1]Columbia University, Center for Climate Systems Research, New York, NY 10025.
Email: bhl7@columbia.edu
[2]Department of the Atmospheric Sciences, The Hebrew University of Jerusalem, Givat Ram, 91904, Jerusalem, Israel. Email: khain@vms.huji.ac.il

1. Introduction

Recent observational and numerical studies demonstrate a significant effect of aerosol particles on precipitation amount and spatial distribution (e.g., Rosenfeld, 1999; Ramanathan et al 2001; Andreae, 2004; Givati and Rosenfeld, 2004; Khain et al 2005, Lynn et al 2005a,b; Jirak and Cotton, 2006). Effects of anthropogenic aerosols produced in urban areas on precipitation are of special interest. Studies have found that air pollution from industrial and urban areas can act to suppress precipitation (Rosenfeld 2000; Borys et. al., 2000). Yet, some work has shown precipitation enhancement around heavily polluted urban areas such as Houston (Shepherd and Burian 2003) and Tokyo (Ohashi and Kida 2002). The difference in the results is possibly related to different environmental conditions in the zones investigated in the studies. As shown by Khain et al (2005), aerosol effects on precipitation from deep convective clouds strongly depends on the thermal stability of the atmosphere, the magnitude of the dominating wind shear, and air humidity. Since urban zones affect both thermal stability and aerosol concentration, the aerosol effects on precipitation can change from location to location. Moreover, since many factors affect precipitation

formation in urban areas, it is difficult to reveal and to quantitatively evaluate effect of aerosols in these areas.

In this sense, investigation of precipitation from topographically produced clouds located downwind of urban areas could provide better opportunity to reveal and evaluate aerosol effects. For instance, Givati and Rosenfeld (2004) examined the effects of air pollution on short-lived shallow clouds, forming over the mountains of California (and Israel) during the cold season. Jirak and Cotton (2006) focused their study on warm season clouds forming at elevated sites downwind of urban areas along the Front Range of California. Each found decreases in precipitation associated with polluted air relative to stations in pristine air of around 30%.

This abstract uses a spectral (bin) microphysics model (SBM) coupled with the Weather Research Forecast (WRF) model to reveal the sensitivity of precipitation from orographic clouds over the Sierra Nevada Mountains to aerosol concentration. A dramatic effect of environmental conditions (mainly relative humidity) on the magnitude and even sign of aerosols on precipitation was found.

These general conclusions are supported in idealized simulations of super-cell storms and squall line development.

2. Experimental Design

To investigate aerosol effects on precipitation, a spectral (bin) microphysical (SBM) scheme has been used that is based on solving an equation system for size distribution functions of drops, three types of ice crystals (dendrites, columns, and plates), snow, graupel and hail/frozen drops as well as aerosol particles. This scheme has been described in detail in Khain et al (2004). Here, the full SBM scheme has been coupled to WRF

(Skamarock et al. 2005) using the same approach for embedding the microphysics within the model dynamic time step as in Lynn et. al (2005a,b).

The coupled model was used to simulate, first, the development of orographic clouds observed during 7 Dec. 2003 (LST) over the Sierra Nevada Mountains. All simulations were produced using a single (non-nested) two-dimensional domain, oriented west to east. Simulations were run for three hours, which was sufficient time for clouds to form on the upslope side of the mountain and to advect over the far mountain peak. The model was run at 6 second time steps using 1 km grid resolution in the horizontal and about 200 m grid resolution in the vertical. **Figure 1** shows the atmospheric initial conditions, while **Fig. 2** shows an example of the extent of cloud cover during the simulation day.

The sensitivity of simulated precipitation to aerosols was tested using two distinct aerosol concentrations, referred to as either "maritime" (Mar) or "continental" (Con). The first represents "clean" air while the second represents "dirty" air. The fields of cloud condensational nuclei (CCN) were initially (t = 0) assumed to be spatially homogeneous. The initial size distribution of CCN was calculated using the method described by Khain et al (2000). Initial dependence of cloud nuclei of super saturation was given by a well-known expression: $N_{CCN} = N_0 S^k$, where S is the super saturation in % (maritime: $N_0 = 250 \text{ cm}^{-3}$, k = 0.462; continental: $N_0 = 1250 \text{ cm}^{-3}$, k = 0.308). The maximum size of dry CCN particles in the continental case was 0.4 μm, which roughly corresponds to a 2 μm radius nucleated droplet. The maximum size of dry aerosol particles in maritime air was assumed equal to 2 μm, which can produce nucleated droplets with radius of about 10 μm. Coefficients N_0 chosen for the experiments provide realistic droplet

concentrations in "continental" (several hundred to thousand cm^{-3}) and maritime (~100 cm^{-3}) conditions. Note that **Figure 3** shows that the distribution of maritime aerosols has a "tail," indicating the presence of relatively large aerosols. At t > 0, the size distribution of aerosols was modified through nucleation scavenging and advection.

Initially, two simulations were conducted, referred to here as Mar-Control and Con-Control, and used the full-microphysics (liquid and ice processes). To investigate the importance of ice processes, simulations were performed with warm microphysics only (no ice processes included). These simulations are referred to as Mar-Control-Liq and Con-Control-Liq, respectively. Sensitivity tests were produced that included increasing the relative humidity from the surface to 2 km to 90%, and from 2 to 5 km to 50%. These were referred to as Mar-RH90 an Con-RH90, respectively. Finally, simulations were done to simulate the effect of background wind on precipitation under both maritime and continental aerosol conditions, referred to as Mar-3/4 and Con-3/4. In these last simulations, the profile of the horizontal wind speed was set equal to ¾ of its initial value in the control. Lastly, simulations with a mixture of aerosols were also produced (referred to as Mar-Con).

The coupled model was also used to simulate the effect of aerosols on super-cell storm development and squall-line development, for both maritime and continental type aerosols.

3. Results: aerosol effects on precipitation from orographic clouds

a. Comparison of Mar-Control with Con-Control

The differences in aerosol concentration led to important differences in the microphysics of the simulated orographic clouds. **Figure 4** shows that maximum droplet

concentration in Con-Control reached greater than 1000 cm^{-3}, while in Mar-Control the droplet concentration did not exceed 100 cm^{-3}. **Figure 5** shows that Con-Control produced much more cloud liquid water (LWC) on the upwind slope, but less rain water content (RWC) than Mar-Control (**Figure 6)**.

Khain et al (2004, 2005) and Lynn et al (2005a, b) simulated deep convective clouds and obtained larger LWC in "polluted" clouds. As explained in these papers, the number of droplets forming in continental air masses is quite large, but because these droplets are relatively small they do not fall as precipitation, but remained suspended in large numbers in clouds and continue growing by diffusion. The same mechanism appears to be effective for relatively shallow orographic clouds as well. Note that cloud droplets in the Con-Control reach higher heights than in Mar-Control because they are small and are able to ascend within cloud updrafts. In comparison, large raindrops formed in Mar-Control fall down before reaching even 1.5 km above the surface.

The Con-Control produced more ice crystals (**Fig. 7**) and snow (**Fig. 8**) then Mar-Control, especially downwind on the mountain slope (and even beyond the highest peak). The higher production of ice crystals and snow content in the Con-Control can be attributed to several factors: first, the process of droplet freezing is not efficient, as stated, in the Con-Control case, since most liquid droplets remain quite small. Thus, in Con-Control most droplets ascend to levels of ~-10- to -20 $^{\circ}$C temperatures. Here, they reach sizes large enough (larger than 10 microns in radius) to be collected by ice crystals (formed by primary ice nucleation, which at these heights reach sizes exceeding ~50 microns through depositional grown). Collision of ice crystals then leads to formation of snow.

In contrast, the Mar-Control simulation produced much more graupel mass (and large frozen drops – not shown) on the first half of the upwind side of the slope than Con-Control (**Fig. 9**). The formation of graupel in the Mar-Control at between x~50 to x~90 km is related to freezing of raindrops at comparatively high temperatures (-5 to -8C). In the Con-Control, the production of graupel is caused mainly by process of riming of ice crystals and snow and is concentrated in the area of the high LWC, snow and ice contents. In both cases, graupel falls on the upwind slope because of significant sedimentation velocity, but it forms and falls further upwind in Mar-Control than Con-Control.

Figure 10 (top-left panel) shows accumulated precipitation (warm+ice) obtained from the Mar-Control and Con-Control, for the three-hour simulation period The figure shows that the maritime simulation produced more precipitation upwind (towards the western boundary or sea) than the simulations with continental aerosols. In fact, the precipitation accumulated in Mar-Control experiment began about 40 km upwind of the starting point of accumulation in Con-Control. Also, the highest amount of precipitation in Mar-Control fell to just to the west of the highest peak, while in Con-Control the largest amount of precipitation fell downwind of the highest peak. **Table 1** shows that the Mar-Control simulation produced about 35% more precipitation than Con-Control.

In total, there are three maxima in the precipitation distribution in Mar-Control, while there are two peaks in the precipitation distribution in Con-Control. Each occurred near local maximum in topography. Based on our analysis of the figures above, the first maximum in Mar-Control's precipitation peak occurred because of warm rain processes. The second maximum occurred mainly because of graupel. Ice crystals and snow induced

the third maximum in the precipitation peak. In Con-Control, warm rain processes did not contribute to precipitation. Rather, the first maximum was formed by graupel, but the amount of graupel in Con-Control was apparently less than in Mar-Control. Both ice and snow processes led to the formation of the second maximum over the highest peak, which was somewhat larger than obtained in Mar-Control.

In both simulations in the third peak, there was sedimentation of crystals, graupel and snow in downdrafts over the eastern side of the peak from stratocumulus-like clouds with cloud base located at or near the surface. Yet, the masses of snow and ice crystals in the Con-Control case were larger and advected further eastwards than in the Mar-Control; thus the precipitation peak is larger in the Con-Control and was shifted further downwind than in the Mar-Control case. The value of the excess was, however, significantly smaller than the deficit in the precipitation in Con-Control over the upwind slope. As a result, the accumulated precipitation in the Mar-Control case turned out to be larger than in the Con-Control case by about 30%, which corresponds well to the observations by Givati and Rosenfeld (2004) and Jirak and Cotton (2006).

The west to east cloud structure obtained in both simulations was punctuated by convective elements west of the highest topographical peak, with stratiform cloud over the peak and downwind. This type of cloud structure is similar to that observed and shown in Fig. 2. Moreover, both simulations produced a sharp cutoff in precipitation amount and cloud mass downwind of the highest peak (as implied by the satellite observation). Also, the Con-Control simulation produced many super-cooled droplets at cloud top, with ice particles present in maximum amount below this level (about 3 km). According to aircraft observations on the same day of these simulations, cloud tops of

smoky clouds contained a large amount of super-cooled droplets, with large amount of ice particles was located below.

The difference in the accumulated rain is related to higher precipitation loss in the Con-Control. For instance, ice crystals and snow penetrating eastward till 180 km contributed to precipitation only slightly, as noted, because of high evaporation within the range 150 km<x< 180 km, where relative humidity was relatively low because of downdrafts leading to air heating. Thus, the important factor in the decrease in the accumulated precipitation in the Con-Control is the higher loss of precipitating mass by ice sublimation in the dry air farther eastward beyond the highest peak and over the downward slope. The concept that the higher loss of precipitating mass in clouds developing in smoky air was also the major mechanism by means of which aerosols can decrease precipitation from deep clouds (as discussed by Khain et al (2005) in detail).

The fields of supercooled water and ice crystals and snow indicate that cloud tops in the Con-Control are higher that in the Mar-Control, so that aerosols invigorate the orographic clouds. This result corresponds to finding by Khain et al (2004, 2005) and Lynn et al (2005a, b) obtained in simulations of deep convective clouds, and reflects the dynamical aerosol effects of aerosols. In the Con-Control case, droplets continue growing by diffusion leading to higher latent heat release as compared to the Mar-Control. Formation of larger amount of ice also leads to higher latent heat release. This leads to higher vertical updraft velocities in the Con-Control as compared to the Mar-Control (**Fig. 11**). Another reason of higher cloud tops in the Con-Control is that both droplets and ice particles are smaller and, having lower sedimentation velocity, are able to ascend to higher levels than in Mar-Control. Consequently, the higher ascent of droplets (and ice

particles) in the continental air mass leads to a greater vertical transport of moisture (as indicated by comparison of the cross-sections of vertical humidity in **Fig. 12**).

b. Comparison of liquid only and mixed-phase microphysics simulations

Figure 10 (right top panel) shows rainfall obtained from Mar-Control-Liq and Con-Control-Liq. Comparing with the corresponding graph in Fig. 10, one notes that the aerosol-induced differences in accumulated precipitation are much larger when ice processes are included. Significant difference in precipitation amounts in the liquid only and mixed phase microphysics with continental aerosols is seen at x~100 km (local topography maximum). Figure 6b indicates that at x~100 km a small amount of warm rain occurred in Con-Control, even when ice microphysics was included. This indicates that collisions between drops start to be efficient to produce warm rain over the first large topographical peak. However, the formation of ice particles by drop-ice collisions actually eliminated warm rain in the Con-Control when ice microphysics was included. Since ice particles formed have lower sedimentation velocity, these particles were advected downwind. Thus, simulation of liquid only processes (without liquid/ice interaction) increases precipitation over the upwind slope and decreases it over downwind slope. Thus, aerosols leading to narrowing the DSD affect significantly not only warm, but also ice cloud microphysics and, accordingly, precipitation distribution and amount.

Figure 10 also shows precipitation from the case with a mixture of maritime and continental aerosols (Mar-Con). The precipitation amount obtained in this simulation was quite similar to with continental aerosols only. Here, the important factor was the number

of droplets rather than the "tail," indicating that the humidity was not high enough to initiate rapid droplet growth of the relatively large nucleated droplets within the droplet spectrum with a high number of nucleated droplets.

c. Sensitivity tests for orographic precipitation.

To investigate the effects of air humidity on orographic precipitation sensitivity tests were produced that included increasing the relative humidity from the surface to 2 km to 90%, and from 2 to 5 km to 50%. These were referred to as Mar-RH90 and Con-RH90. Cloud microstructure also depends on vertical velocities and wind speed; these experiments were referred to as Mar-3/4 and Con-3/4.

Effects of wind speed. Decreasing the wind to 3/4 of its initial value reduced the amount of precipitation in both Mar-3/4 and Con-3/4 (Figure 10 (left bottom panel)). This is because a decrease in the horizontal velocity led to a corresponding decrease in the vertical velocity over upwind slope. Each simulation produced two peaks in precipitation, and Con-3/4 produced precipitation even near the beginning of the upwind slope. Because there were smaller vertical velocities, the droplet concentration was smaller in Con-3/4 than in Con-Control (not shown), which allowed for the production of even warm rain in the polluted air. However, the amount of precipitation was much less (Table 1) and shifted downwind because rain-drop formation took a longer period of time. In the simulation with mixed aerosols, the results were still quite similar to with continental aerosols.

Effects of air humidity. Increasing the relative humidity led to a shift of precipitation formation westward (Fig. 10 right bottom panel) to x~30 to 35 km in both maritime and continental simulations. Moreover, amounts are quite similar. Clouds formed near the

underlying surface (**Fig. 13**). Since the slope was quite gentle at x ranged from 0 to 30 km, the vertical velocity at cloud base was less than ~1 m/s, and super saturation was less in the cloud updrafts (not shown) than in the control simulations. This led to a relatively low droplet concentration even in Con-RH90, that varied from several tens near cloud base to several hundred at 1-1.5 km above the underlying surface (**Fig. 14**). This means that there was a wide spectrum even in the continental case. Such cloud structure fosters droplet collisions (and this simulation produced more precipitation than Mar-Control, Table 1), since droplet concentration was not high and the DSD contained large droplets nucleated near the cloud base. Moreover, high humidity dramatically decreased evaporation of falling droplets. As a result, the increase in the air humidity led to warm rain formation in Con-RH90 (as well as Mar-RH90) (**Fig. 15**), although still less than in the latter.

Even though cloud rain water mass contents were more similar on the upwind side of the mountain slope, the Con-RH90 simulation still produced quite more ice mass content on the upwind slope (**Fig. 16**). This led to greater production of snow mass content in Con-RH90 over the mountain peak as compared to Mar-RH90 (**Fig. 17**). Mar-RH90 did, however, still produce more graupel than Con-RH90 (**Fig. 18**). Hence, the microphysical pathways leading to precipitation were still different: with warm rain and graupel formation in RH90 being more important than precipitation from snow.

4. Results: Super-cell formation

Simulations were produced with a 3-D version of WRF-SBM for simulation of an idealized supercell storm, using "maritime" and "continental" aerosols with characteristics similar to those used for simulation of orographic clouds. Two values of

relative humidity were used: with relative humidity initially set to > 90%, and with relative humidity set to < 75% in the boundary layer. It is clear that precipitation increases with the increase in the air humidity in both cases. As concerns to aerosol effects, it is remarkable that the sign of the difference in the accumulated precipitation depends on the air humidity. **Figure 19** shows that with high relative humidity, the simulation with continental aerosols produced more accumulated precipitation than the simulation with maritime aerosols. However, the simulation with maritime aerosols produced somewhat more precipitation than the simulation with continental aerosols at lower relative humidity (**Fig. 20**). This result again supports the general conclusions reached by Khain et al (2005) from the budget analysis that increase in the aerosol concentration decreases precipitation from cloud systems when precipitation loss is significant, i.e. when precipitating particles fall through relatively dry environmental air.

The results of simulations indicate significant aerosols effects on the spatial pattern of precipitation within super-cell storms. The simulation with maritime aerosols produced the heaviest amount of precipitation in the southern flank of the storm. With continental aerosols, however, the heaviest precipitation was "twisted" to the north and east of the "nose" of the precipitation shield.

The relative shift in the spatial distribution of precipitation in the simulated supercell storms is caused by aerosol effects on cloud dynamics and microphysics. In the simulation with continental aerosols, a delay in raindrop formation, as well as higher vertical velocity, allowed cloud hydrometeors to ascend to higher levels with different wind direction. As a result, liquid and ice mass were advected in the counterclockwise direction in the "continental" supercell storm and then fall farther to the "north" and

"east" within the simulation domain. The elongated tail on the continental simulations occurred because droplets reached higher heights and froze, with the production of a number of small ice and snow particles having low sedimentation velocity (not shown).

5. Results: Squall-line formation

The purpose of these simulations was two-fold: a) to reveal effects of aerosols on precipitation, and b) to reveal effects of ice processes in cloud-aerosol interaction.

The sensitivity of the precipitation amounts to aerosol concentration depended on whether the simulations were produced with liquid only or mixed phase (ice and liquid) microphysical processes. When mixed phase and ice processes were excluded, the simulation with "continental" aerosol concentrations produced more precipitation than the simulation with "maritime" aerosols.   In contrast, the simulation with maritime aerosols produced more precipitation than the continental simulation when including mixed phased processes (**Figure 21**).

The results can be explained as follows. The simulation with continental aerosols produced many more droplets than that with maritime aerosols. These droplets ascended in the squall line updraft, with some eventually growing large enough to lead to droplet coalescence. Because it takes longer for droplets in the updraft to reach the appropriate size to produce raindrops, the droplets ascended higher and release more latent heat than droplets in the simulation with maritime aerosols. Hence, the updraft was more vigorous and cloud mass amount larger than in the maritime simulation. The invigoration of convection by aerosols was found reported by Khain et al (2005), Lynn et al (2005), as well in the simulations discussed above. It seems that humidity was high enough in these

13

simulations, so that clouds in the "continental" squall line with warm microphysics realized a higher precipitation "potential."

However, with mixed phase and ice processes turned on, the "continental" clouds produce much more ice and snow particles than the maritime ones (not shown). This ice was then advected downwind, where the cloud ice mass was "lost" to evaporation in downdrafts. Thus the loss of precipitating mass turns out to be larger in "continental" squall line. In comparison, the simulation with maritime aerosols produced large ice particles (e.g., graupel and hail), having larger sedimentation velocity and leading to greater rain production than in the simulation with continental aerosols.

Note that ice formation significantly decreased accumulated rain in both cases because of a stronger residential time of ice particles and their higher lost by sublimation.

6. Conclusions

Spectral (bin) Microphysics was coupled with a 2-d version of the Weather Research Forecast model and used to investigate aerosol effects (pollution) on amount and spatial distribution of precipitation in the Sierra Nevada Mountains, in super-cell formation, and 2-d squall-line development. Two types of microphysical situations were simulated, the first with low concentration maritime aerosols (clean-air) and second with high concentration continental aerosols (dirty-air). The continental aerosol simulation was designed to reproduce the effect of anthropogenic aerosols produced in upwind urban areas on downwind precipitation forming on the mountain slope, in the super-cell, and squall-line. The maritime aerosol simulation reproduced precipitation forming in pristine air. After three hours of simulation, precipitation amount in the maritime simulation was about 30% larger on the upwind slope than in the simulation with continental aerosols.

Mixing maritime and continental aerosol distributions gave very similar results to those of continental aerosols alone. In the super-cell, the heaviest precipitation fell further to the "north" and "east," while in the squall-line the exclusion or inclusion of ice phase processes was the key as to whether more or less precipitation fell in continental versus maritime simulations.

In the orographic simulations, the maritime simulation produced warm rain near the beginning of the upwind slope, while the continental simulation did not produce warm rain anywhere on the slope. The maritime simulation also produced some warm rain, but mostly graupel precipitation in a second maximum occurring further up the mountain slope above a topographical peak. The continental simulation produced less graupel in the same location and less precipitation. This simulation, however, produced more ice and snow than the maritime simulation, which accumulated in larger amounts on the highest peak and downwind. Owing to the greater production of ice and snow, the maximum amount of precipitation on the highest topographical peak was shifted downwind from the location of maximum precipitation in the maritime simulation. Both simulations had convective-type precipitation on the upwind slope, which transitioned to stratiform precipitation further up the mountain slope. Evaporation of ice and snow in atmospheric downdrafts beyond the highest peak led to a sharp cutoff in precipitation downwind of this peak, similar to what was shown in an observed satellite photograph.

As noted, the simulation with continental aerosols produced more ice and snow particles than the simulation with maritime aerosols, without producing warm rain. Clouds forming in the continental aerosol air turn out to be more vigorous and reached higher heights than those formed in clean air, with ice crystals and snow within that had

lower sedimentation velocities than raindrops and graupel. This led to a shift of ice precipitation downwind in the simulation with continental aerosols compared to warm rain precipitation and graupel type precipitation in the maritime simulation. These ice and snow particles were advected by the background wind, and, as noted, evaporated on the downwind side of the highest mountain peak. Because ice and snow particles were evaporated, the simulation with continental aerosols produced less precipitation over the whole mountain slope, owing to the greater prevalence of these types of precipitation particles in this simulation than in the maritime simulation. According to statistical analysis (Givati and Rosenfeld 2004; Jirak and Cotton 2006) anthropogenic aerosols lead to a decrease of precipitation over mountain region by about 30% and to a shift of precipitation downwind of polluted urban centers. Our results also indicated a similar decrease in precipitation amount, etc, as noted above.

When a mixture of aerosols was used, there was added both small and large aerosols to the continental aerosol distribution. Even though there were some large cloud droplets formed, they could not grow sufficiently to lead to rapid rainwater content production.

Supplemental simulations with ice microphysics excluded revealed a crucial role of ice formation in the aerosol effects on precipitation. Without simulated ice processes, the simulation with continental aerosols produced more precipitation in the location of the first topographical peak than it did when ice processes were included. Yet, the precipitation amount in the maritime simulation did not show similar sensitivity to the inclusion or exclusion of ice processes. This further emphasizes the importance of drop size distribution on the size distribution and types of ice particles that formed in each

simulation. Thus, ice formation significantly intensifies the effects of aerosols on the precipitation amount and spatial distribution.

In sensitivity tests, we identified relative humidity and wind speed as critical environmental factors that determined both precipitation amounts and relative differences between simulations in clean and dirty air. Higher humidity decreased the cloud base level and triggered the cloud formation further upwind on the mountain slope where vertical velocity was smaller than further downwind on the slope. As a result, droplet concentration turned out to relatively small, and droplet spectra distributions were able to develop to produce raindrops. Effective warm rain formation than occurred even in the continental aerosol case. Also, high relative humidity reduces precipitation loss caused by drop and ice evaporation. Thus, the increase in air relative humidity decreased the difference in precipitation amounts between the clean- and dirty-air simulations, and even changed the sign of this difference.

A decrease in the speed of the background wind led to decrease in the vertical velocity and to a delay in the cloud and precipitation formation. Even so, the maritime precipitation formed earlier, and somewhat further up the mountain slope and in greater amounts than in the continental simulation.

The main result of these idealized simulations is the revealing of aerosol effects on the precipitation formation and distribution from orographic clouds, as well as revealing the most important microphysical and environmental factors that can enhance or inhibit the aerosol effects.

Significant aerosol effects on precipitation rate, precipitation amount and spatial distribution were found in 3-D simulations of super-cell storms. In super-cell simulations,

the greater vertical transport of moisture in the simulation with continental aerosols leads to advection of cloud mass and hence precipitation into the northeast quadrant of the storm. A dramatic effect of air humidity was demonstrated. When the higher relatively humidity was used in the model simulations, there was more accumulated rain in both maritime and continental simulations than with lower relative humidity. A larger increase in precipitation in the continental simulation as compared to the maritime one,, suggests, however, that humidity decreased precipitation loss more so in the continental simulation than the maritime one.

A dramatic effect of ice processes on cloud-aerosol interaction was found in simulations of a squall line. In 2-d squall line simulations without ice processes, more precipitation occurs in the continental aerosol simulation, but with ice processes included the simulated ice mass is "lost" downwind of the precipitating cloud.

References:

Andreae, M.O., D. Rosenfeld, P. Artaxo, A.A. Costa. G.P. Frank, K.M. Longlo, and M.A.F. Silva-Dias, 2004: Smoking rain clouds over the Amazon. Science, 303, 1337-1342.

Borys, R. D., D. H. Lowenthal, and D. L. Mitchell, 2000: The relationships among cloud microphysics, chemistry, and precipitation rate in cold mountain clouds. *Atmos*. *Environ., * **34**, 2593–2602.

Givati A. and D. Rosenfeld , 2004: Quantifying precipitation suppression due to air pollution. *J. Appl. Meteorol.* 43, 1038-1056.

Jirak I. L. and W. R. Cotton. 2006: Effect of Air Pollution on Precipitation along the Front Range of the Rocky Mountains. *J. Appl. Meteorol. and Climatol*, 45, No. 1, pp. 236–245.

Khain, A. P., M. Ovtchinnikov, M. Pinsky, A. Pokrovsky, and H. Krugliak, 2000: Notes on the state-of-the-art numerical modeling of cloud microphysics. *Atmos. Res.* 55, 159-224.

Khain A. P., D. Rosenfeld and A. Pokrovsky, 2001: Simulation of deep convective clouds with sustained supercooled liquid water down to –37.5 C using a spectral microphysics model. *Geophysical Research Letters*, 3887-3890.

Khain A., A. Pokrovsky and M. Pinsky, A. Seifert, and V. Phillips, 2004: Effects of atmospheric aerosols on deep convective clouds as seen from simulations using a spectral microphysics mixed-phase cumulus cloud model Part 1: Model description. *J. Atmos. Sci 61, 2963-2982.*

Khain A. and A. Pokrovsky, 2004: "Effects of atmospheric aerosols on deep convective clouds as seen from simulations using a spectral microphysics mixed-phase cumulus cloud model Part 2: Sensitivity study", *J. Atmos. Sci. 61, 2983-3001*

Khain, A. D. Rosenfeld and A. Pokrovsky 2005: Aerosol impact on the dynamics and microphysics of convective clouds. *Q. J. Roy. Meteor. Soc.* 131, 2639-2663

Kovetz, A. and Olund, B., 1969: The effect of coalescence and condensation on rain formation in a cloud of finite vertical extent. *J. Atmos. Sci.,* 26, 1060-1065

Lynn *B*., A. Khain, J. Dudhia, D. Rosenfeld, A. Pokrovsky, and A. Seifert *2005:* Spectral (bin) microphysics coupled with a mesoscale model (MM5). Part 1. Model description and first results*. Mon. Wea. Rev.* 133, 44-58.

Lynn *B*., A. Khain, J. Dudhia, D. Rosenfeld, A. Pokrovsky, and A. Seifert *2005:* Spectral (bin) microphysics coupled with a mesoscale model (MM5). Part 2: Simulation of a CaPe rain event with squall line *Mon. Wea. Rev.* , 133, 59-71.

Ohashi Y. and H. Kida, 2002: Local Circulations Developed in the Vicinity of Both Coastal and Inland Urban Areas: A Numerical Study with a Mesoscale Atmospheric Model, *J. Appl. Meteorol,41,.30-45*

Ramanathan , V., P.J. Crutzen, J. T. Kiehl, D. Rosenfeld, 2001: Aerosols, climate and the hydrological cycle. Science, 294, 2119-2124.

Rosenfeld, D., 1999: TRMM observed first direct evidence of smoke from forest fires inhibiting rainfall. Ge*ophys. Res. Lett.,* 26, 20, 3105.

Rosenfeld, D, 2000: Suppression of rain and snow by urban and industrial air pollution. *Science,* 287 (5459), 1793-1796.

Shepherd, J. M., and S. J. Burian, 2003: Detection of urban-induced rainfall anomalies in a major coastal city, *Earth Interactions*, **7**, 1-14.

Skamarock, W., J.B. Klemp, J. Dudhia, D. O. Gill, D. M. Barker, W. Wang, J.G. Powers, 2005: A description of the Advanced Research WRF Version 2, NCAR Technical Note, June 2005, Mesoscale and Microscale Meteorology Division, NCAR, Boulder, Colorado, USA.
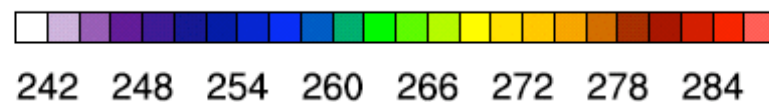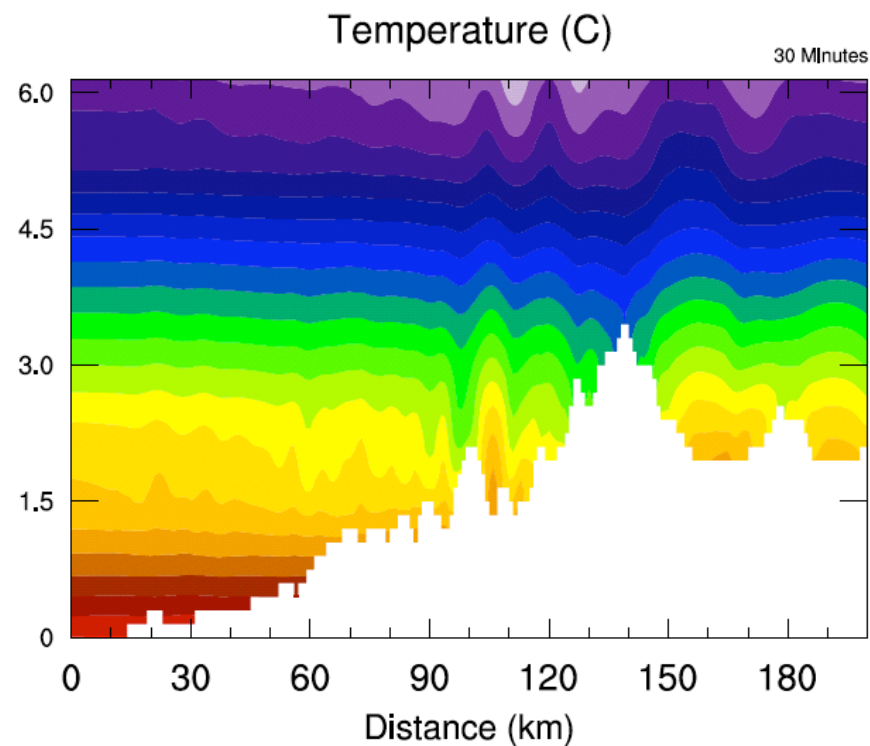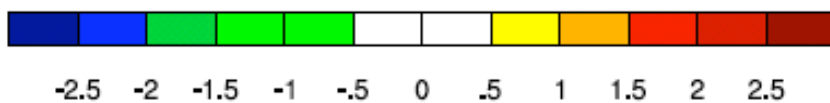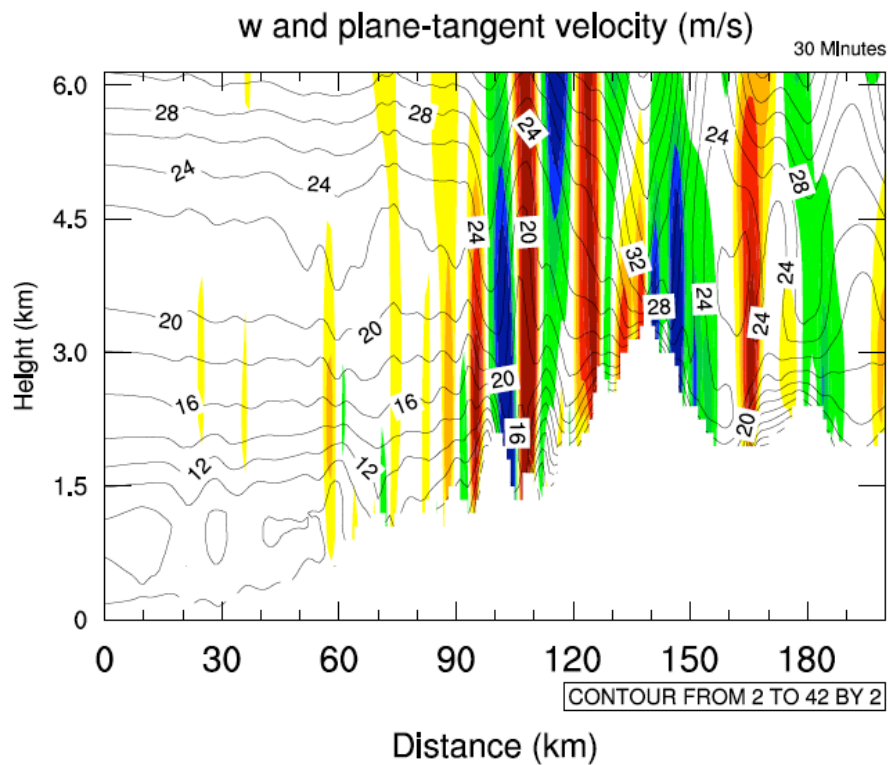
Figure 1: West to east cross-sections of vertical velocity and horizontal wind (left panel), temperature (right panel), and relative humidity (next page) 30 minutes after the start of the simulations. The figures show 201 grid elements, stretching from X=150 to X=350 km.
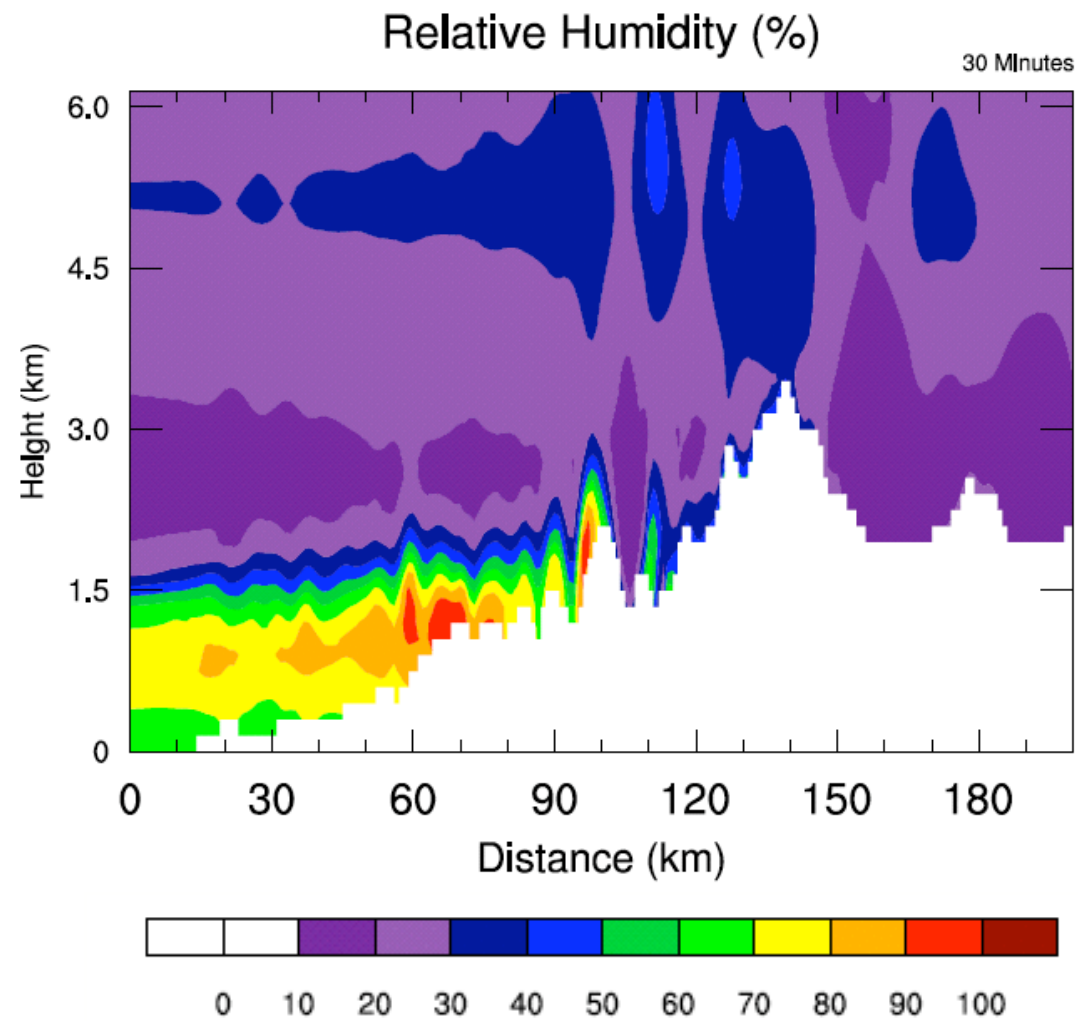
Figure 1: Continued from previous page.
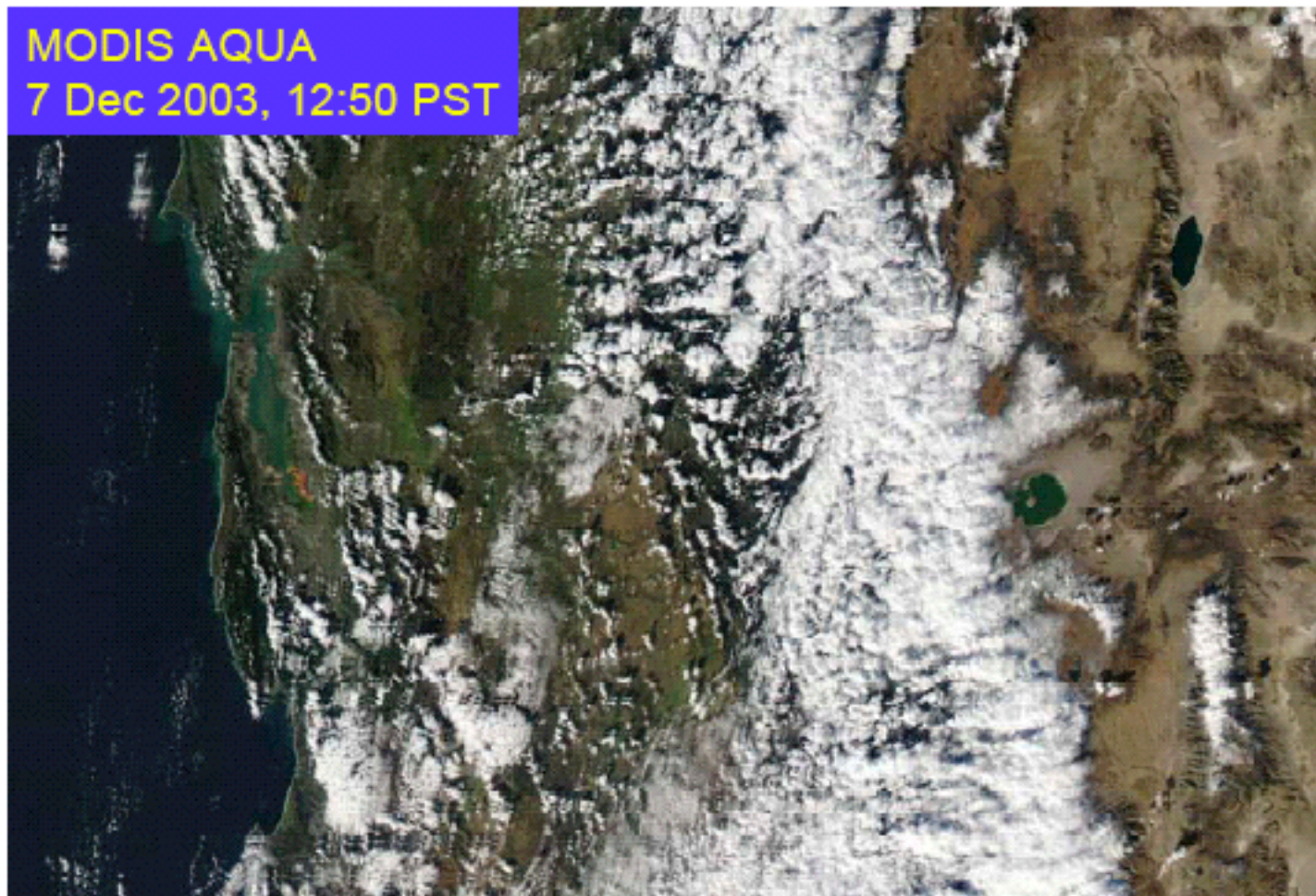
Figure 2: Satellite picture of the cloudiness during smoky conditions (7 Dec. 2003). One main peak of cloudiness and sharp eastern boundary of cloudiness is seen. Clouds are small convective or stratocumulus clouds.
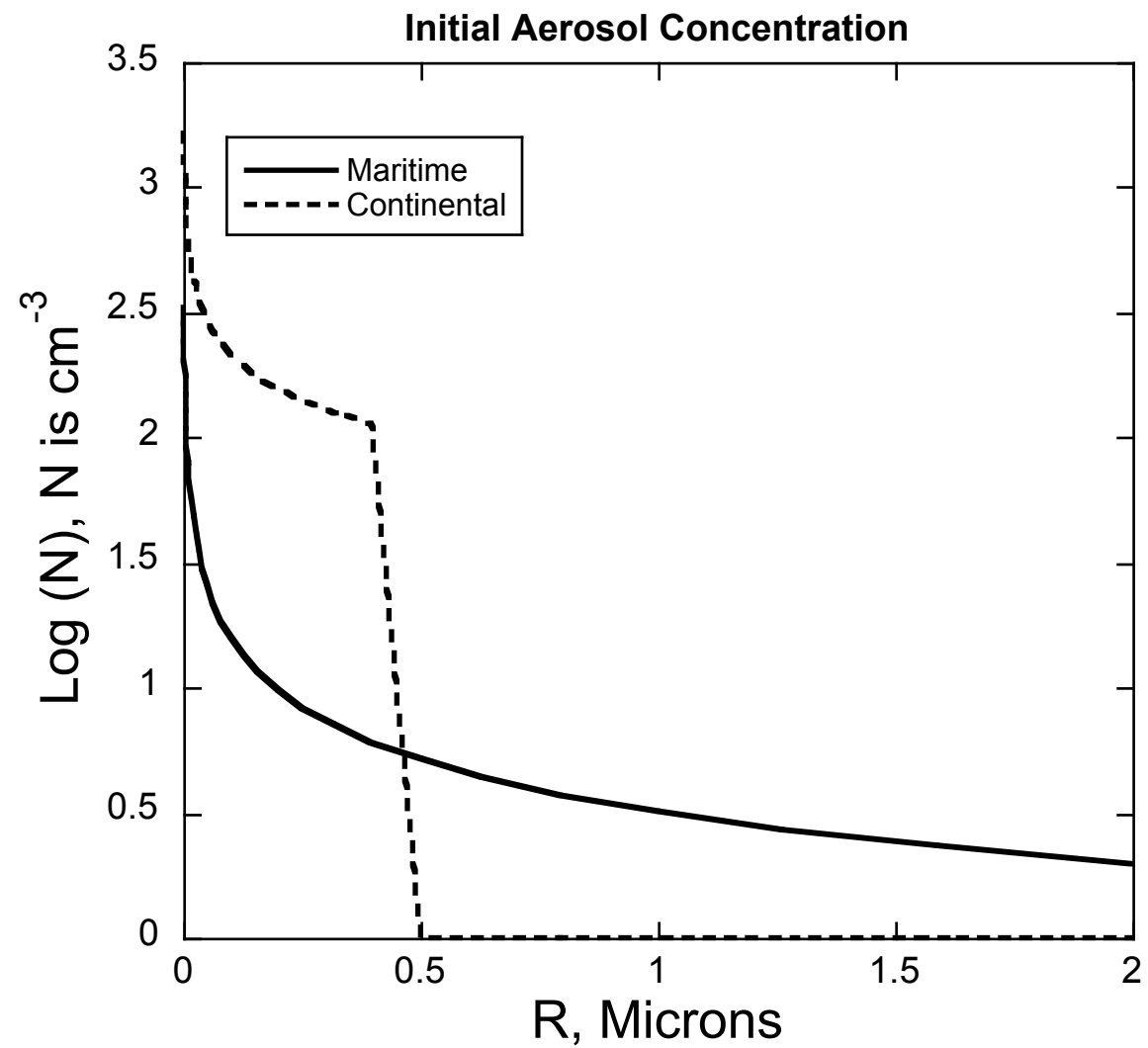
Figure 3:Size distribution of aerosols from maritime and continental simulations.
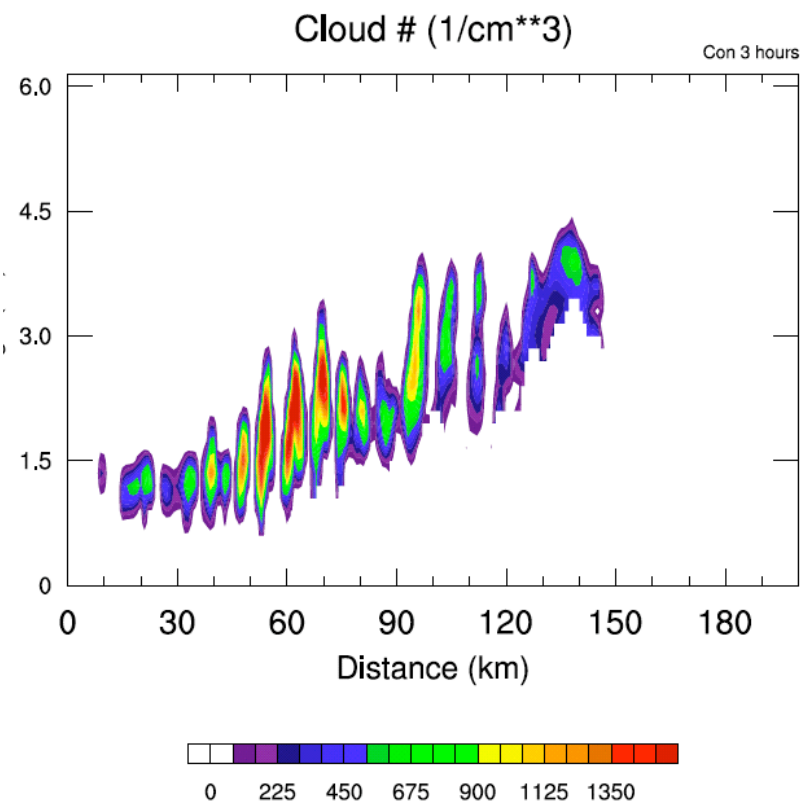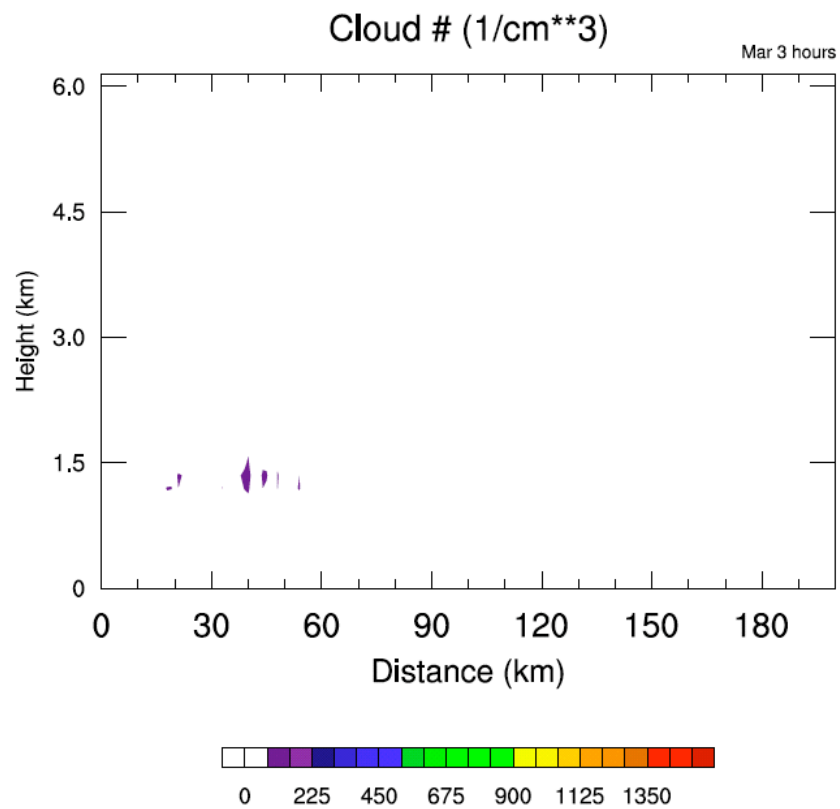
Figure 4: West to east cross-sections of cloud droplet concentration simulated with MAR-Control (left) and Con-Control (right) at 3 hours.
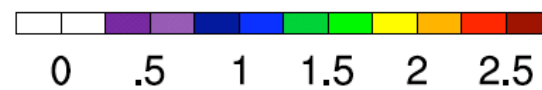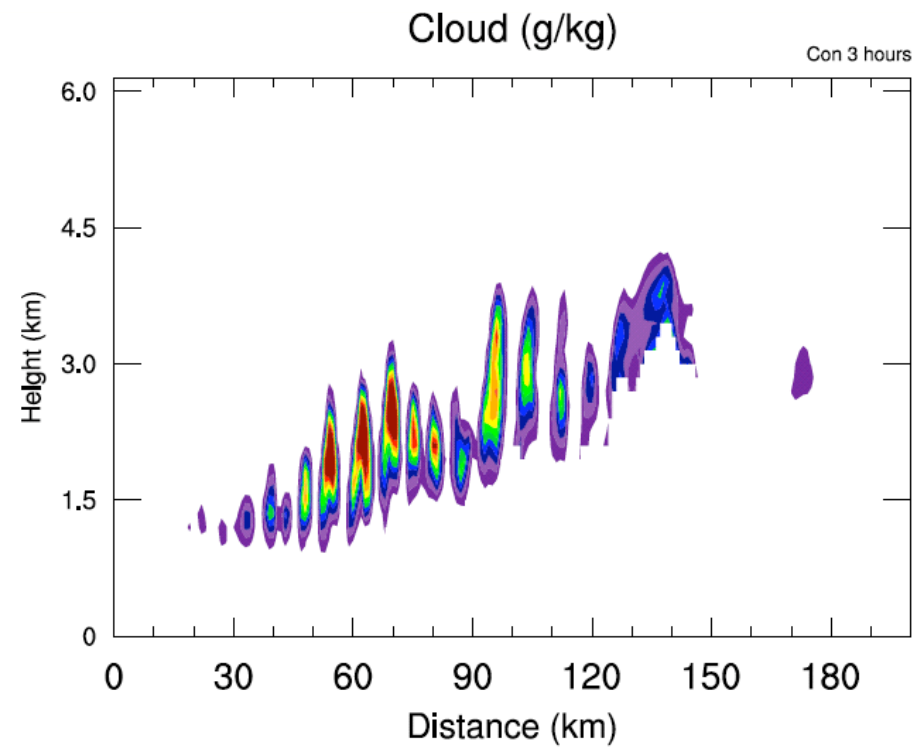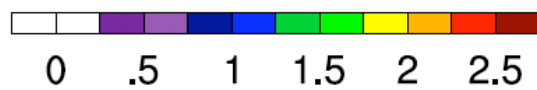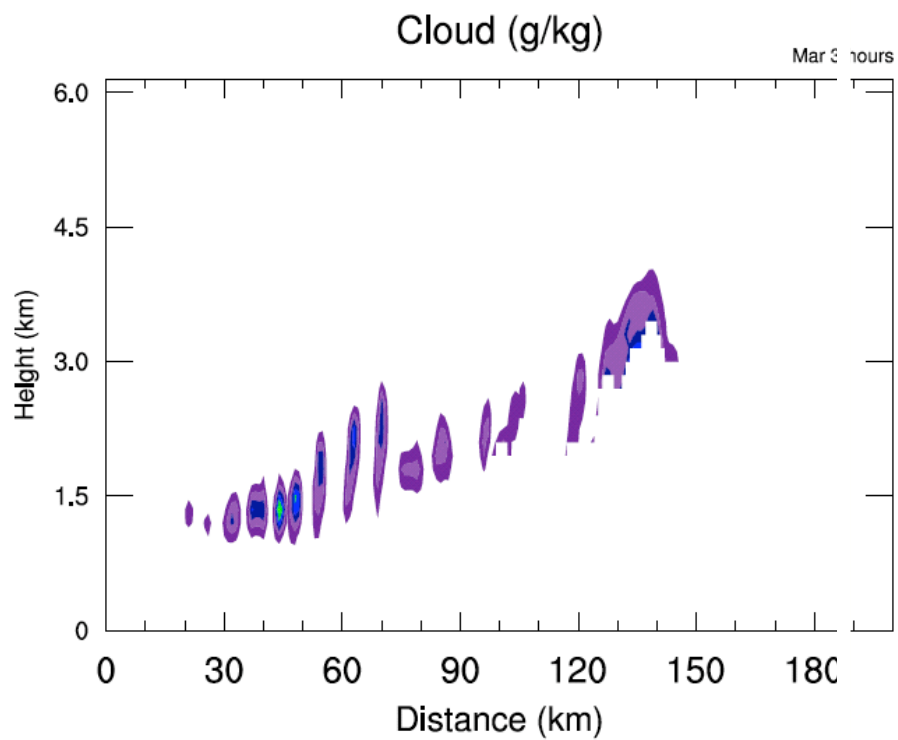
Figure 5: West to east cross-sections of cloud water content simulated with MAR-Control
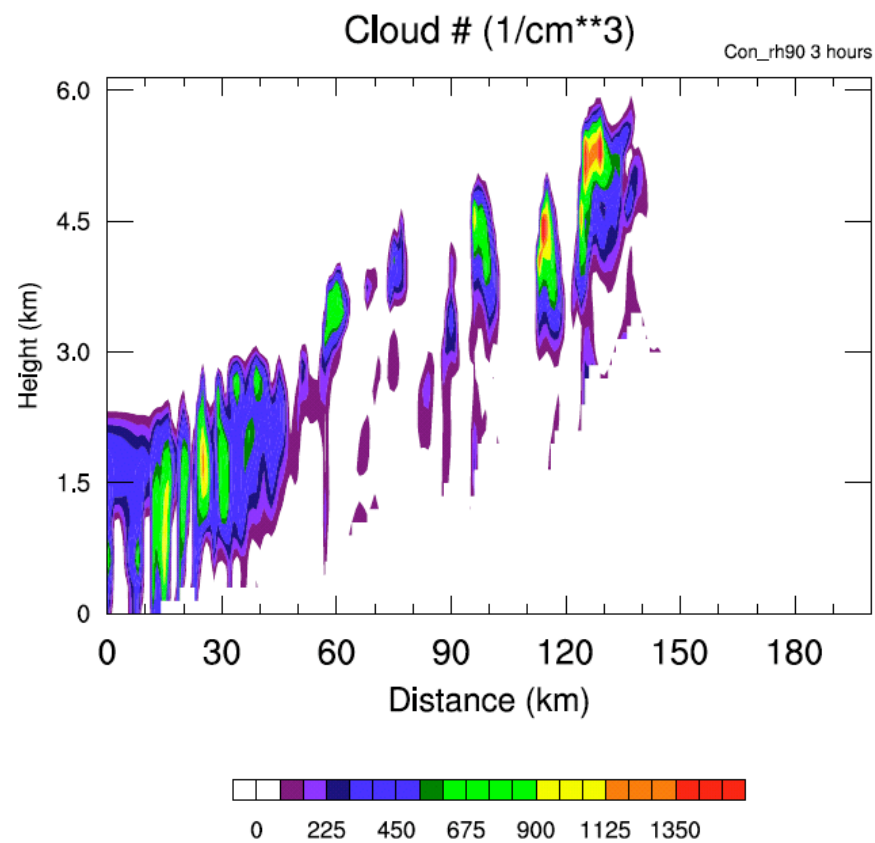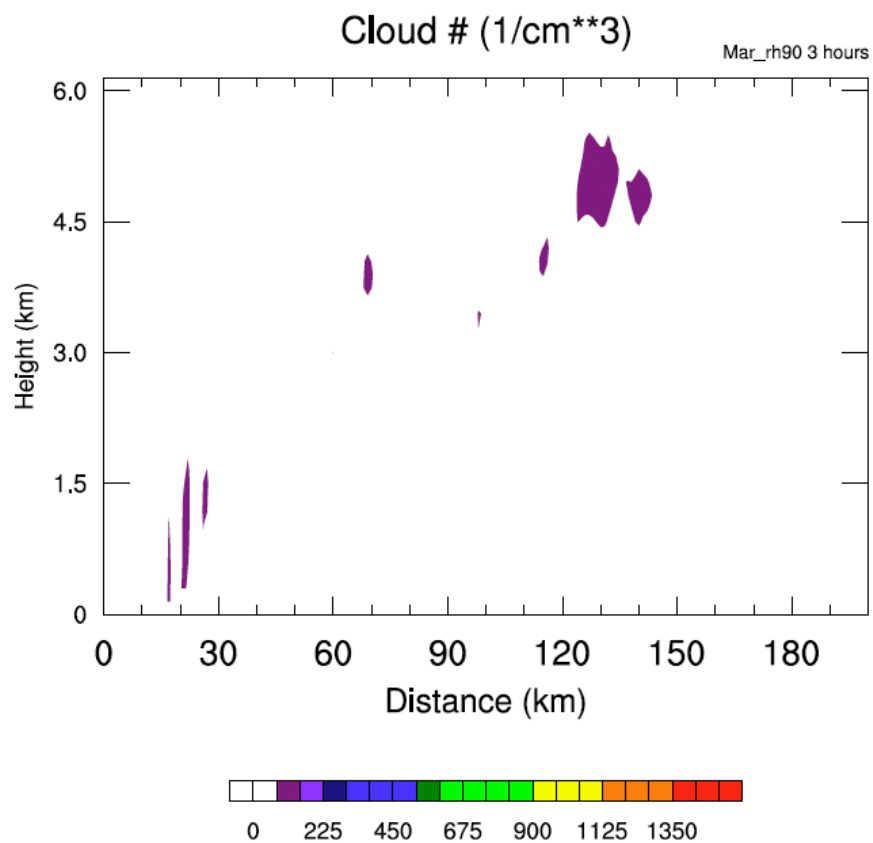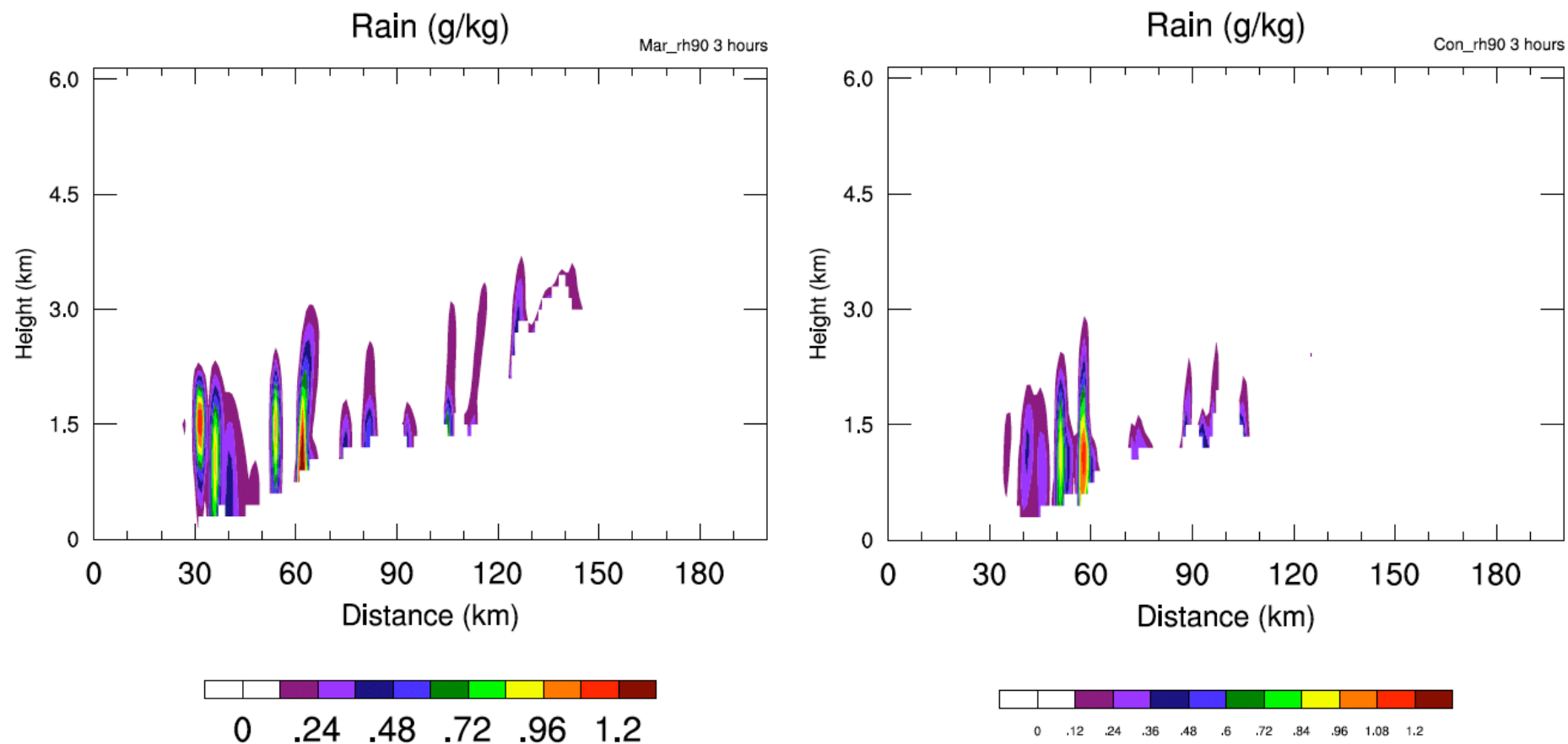(left) and Con-Control (right) at 3 hours.
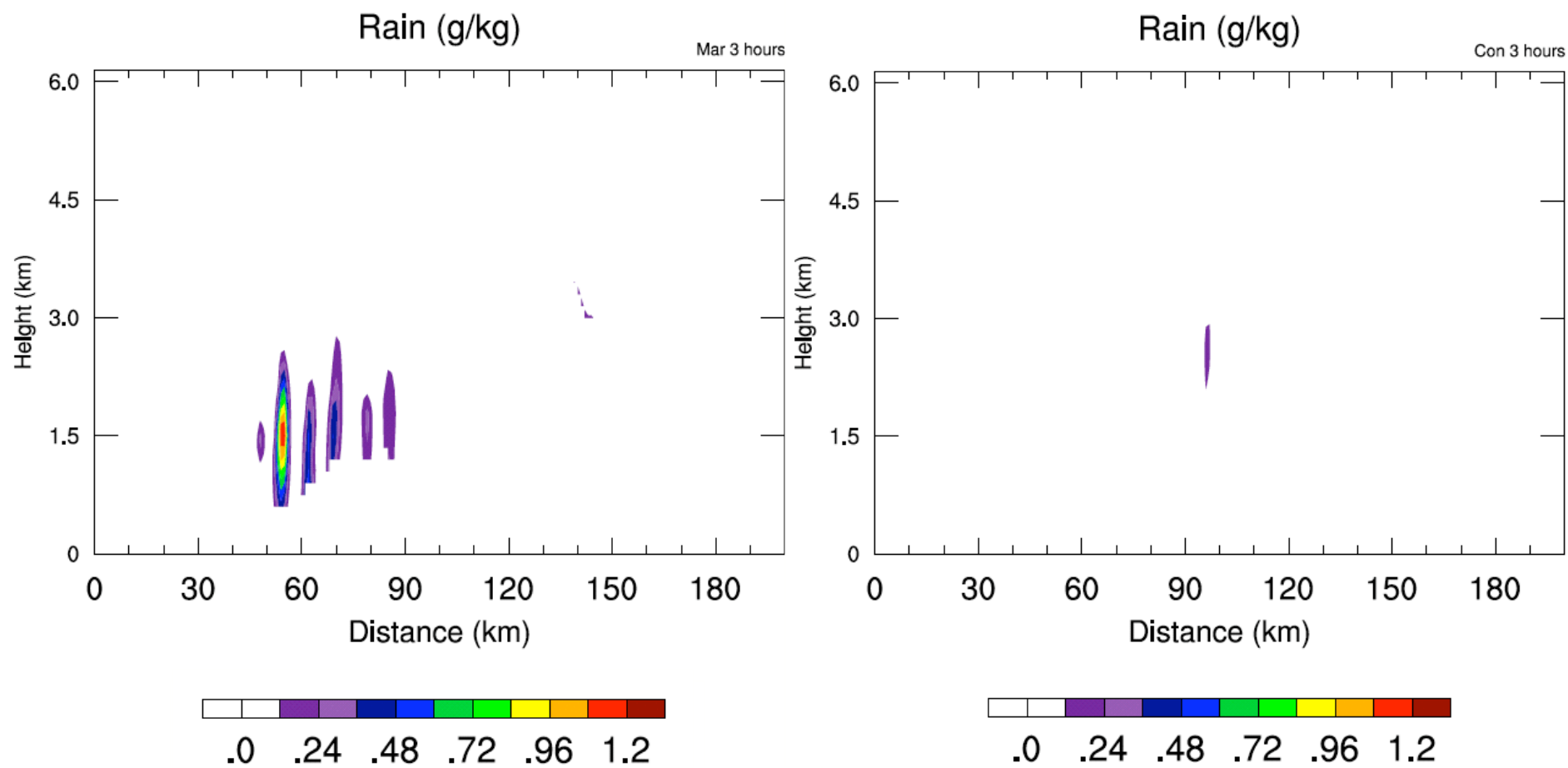
Figure 6: West to east cross-sections of cloud rain content simulated with MAR-Control (left) and Con-Control (right) at 3 hours.
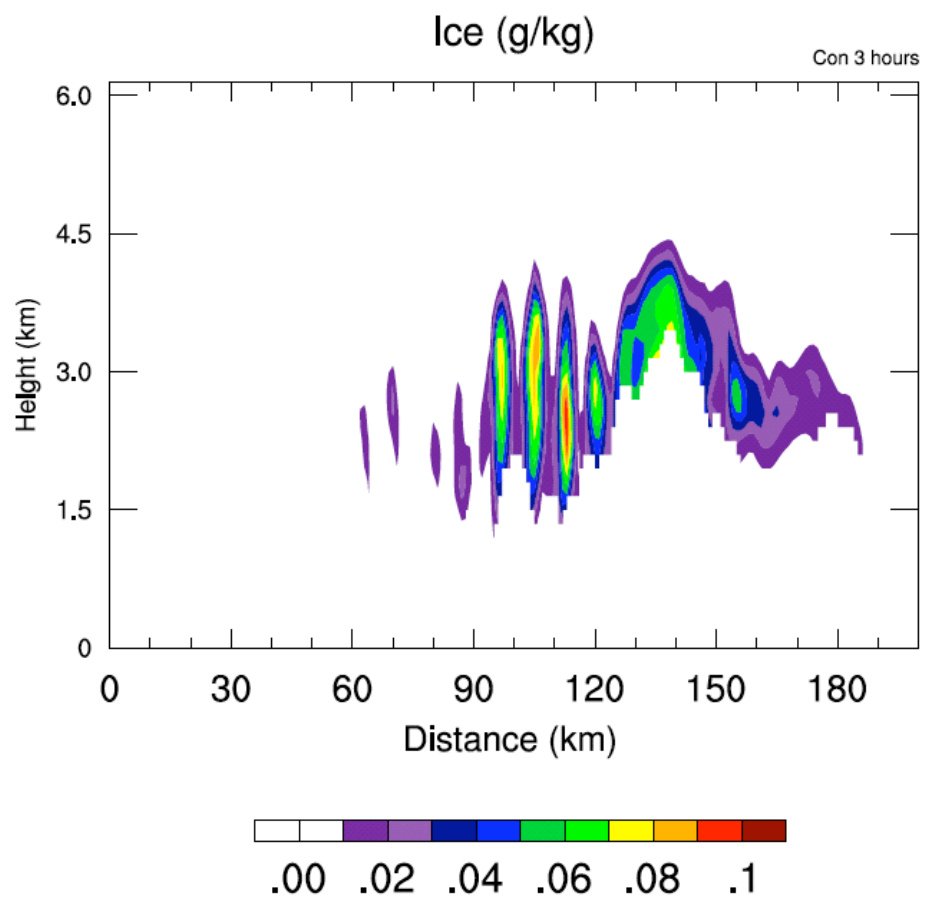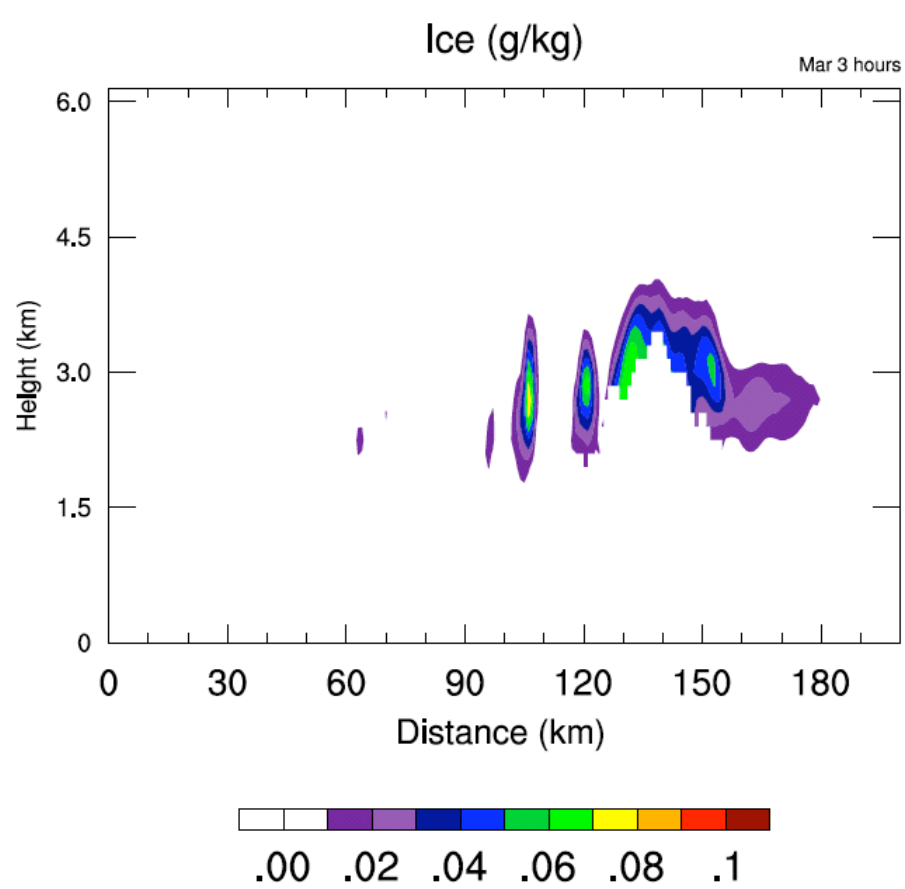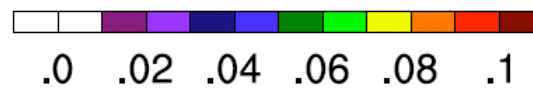
Figure 7: West to east cross-sections of cloud ice content simulated with MAR-Control (left) and Con-Control (right) at 3 hours.
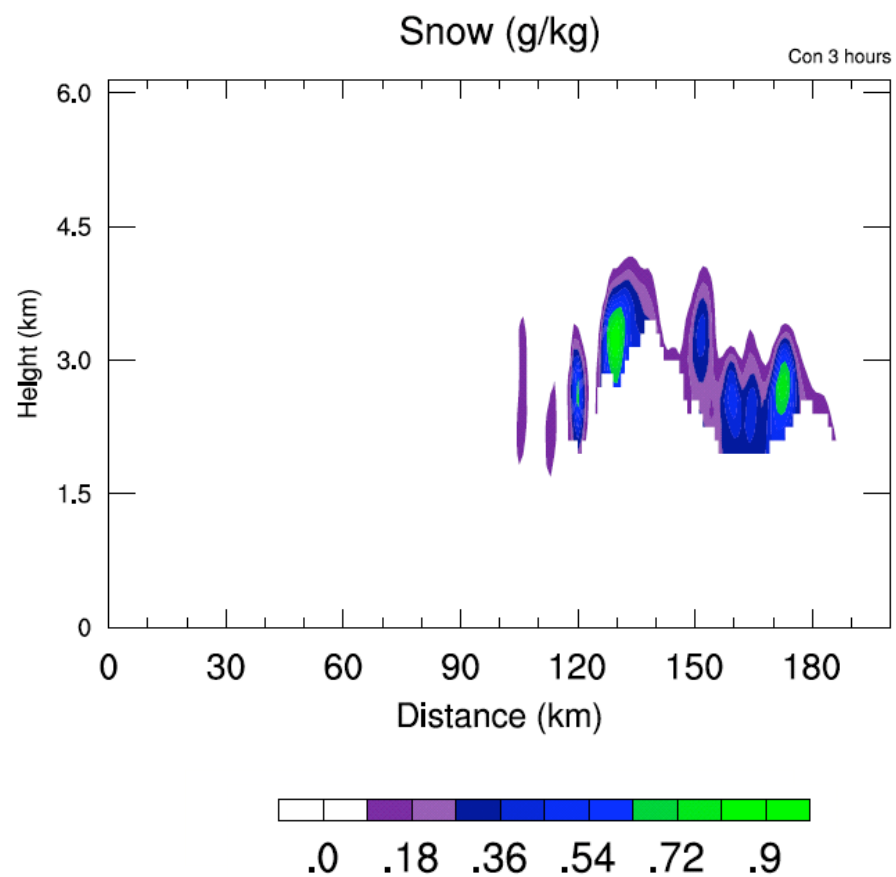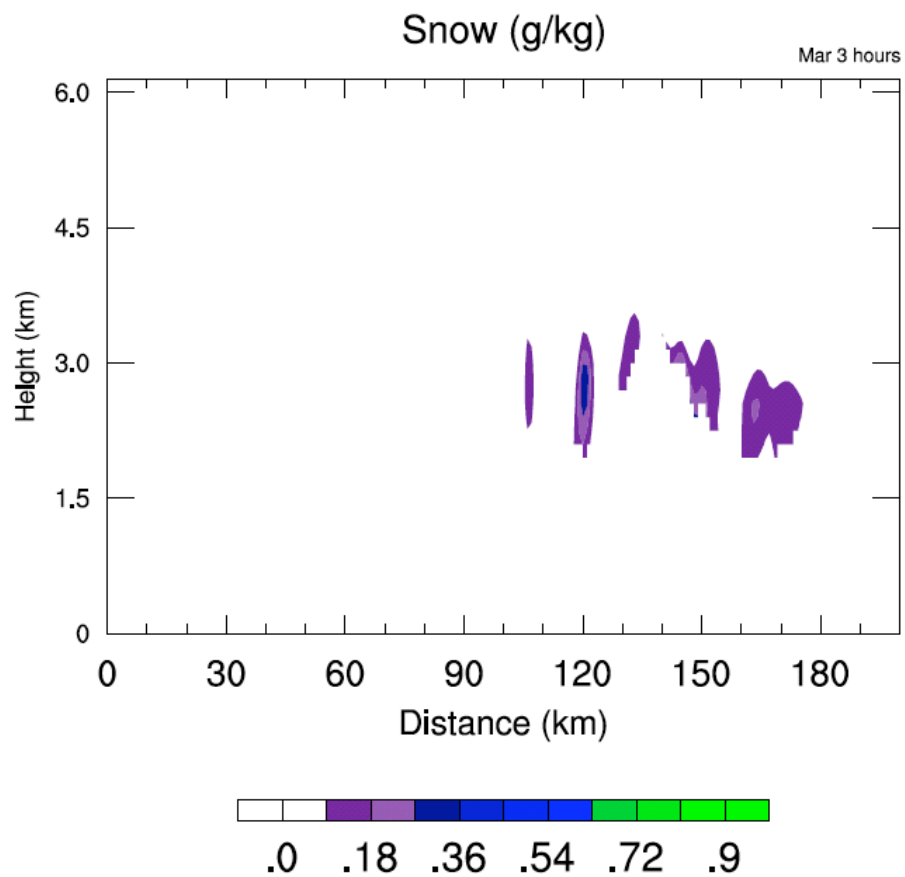
Figure 8: West to east cross-sections of cloud snow content simulated with MAR-Control (left) and Con-Control (right) at 3 hours.
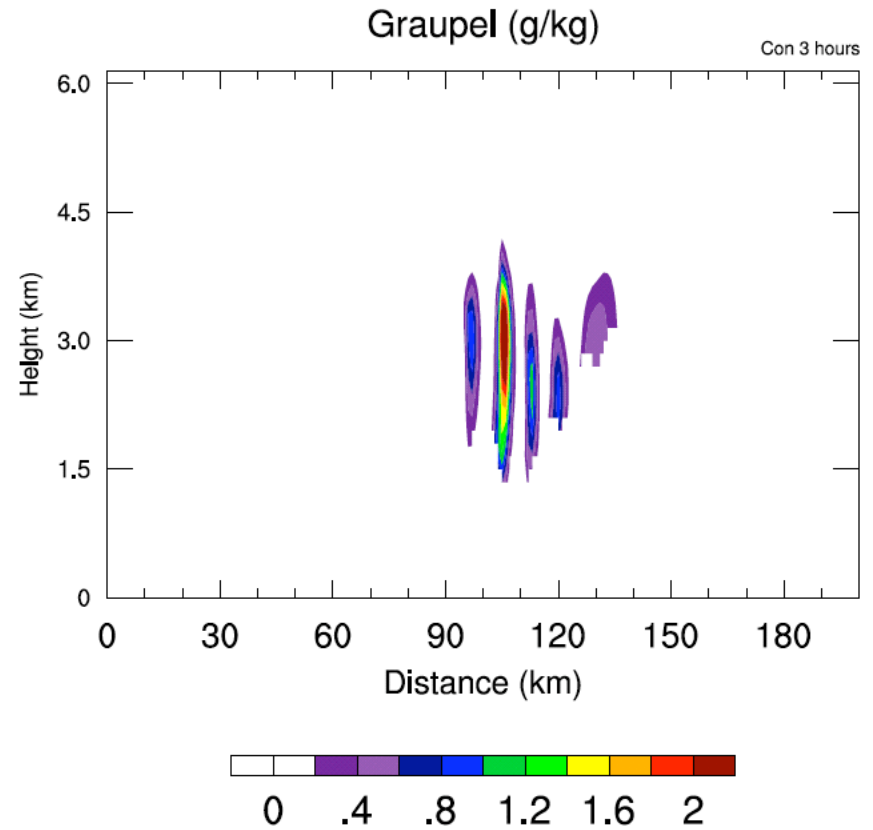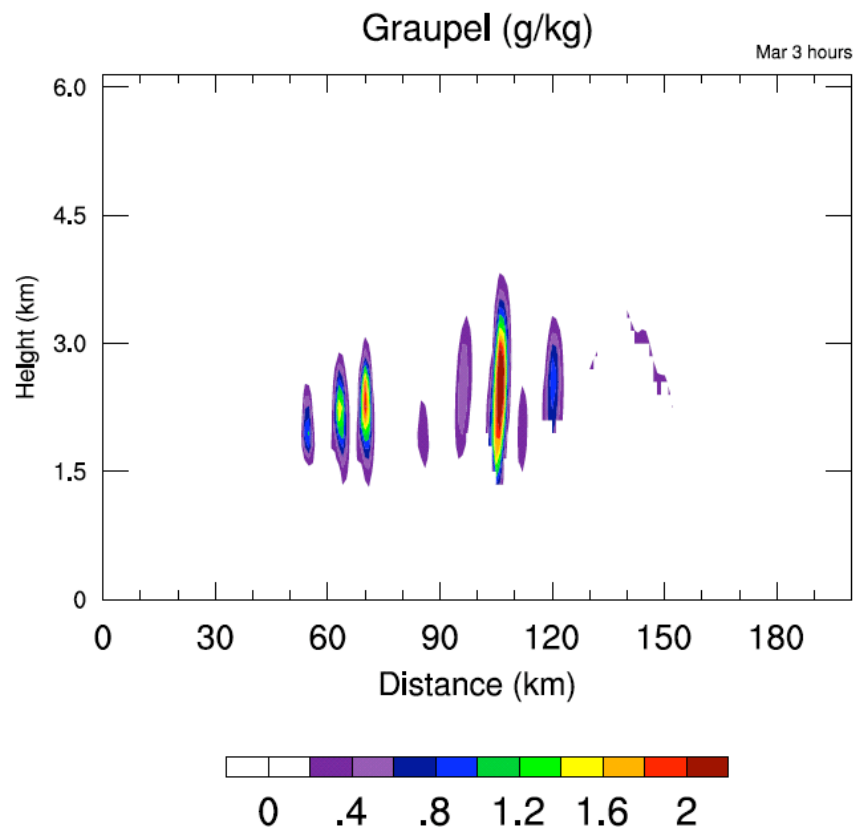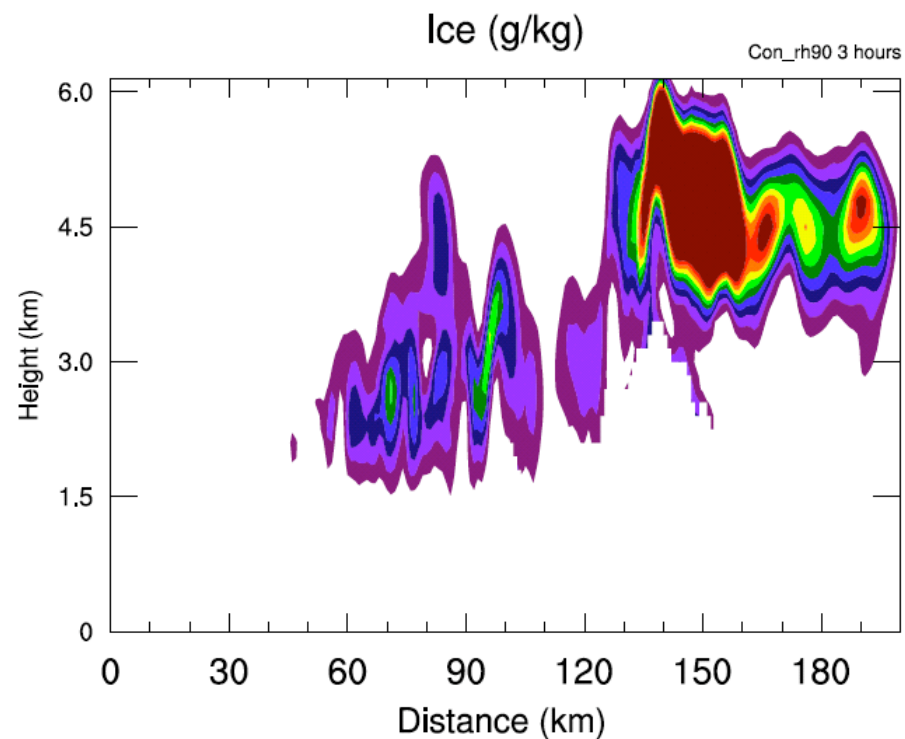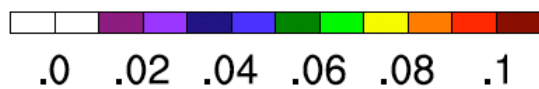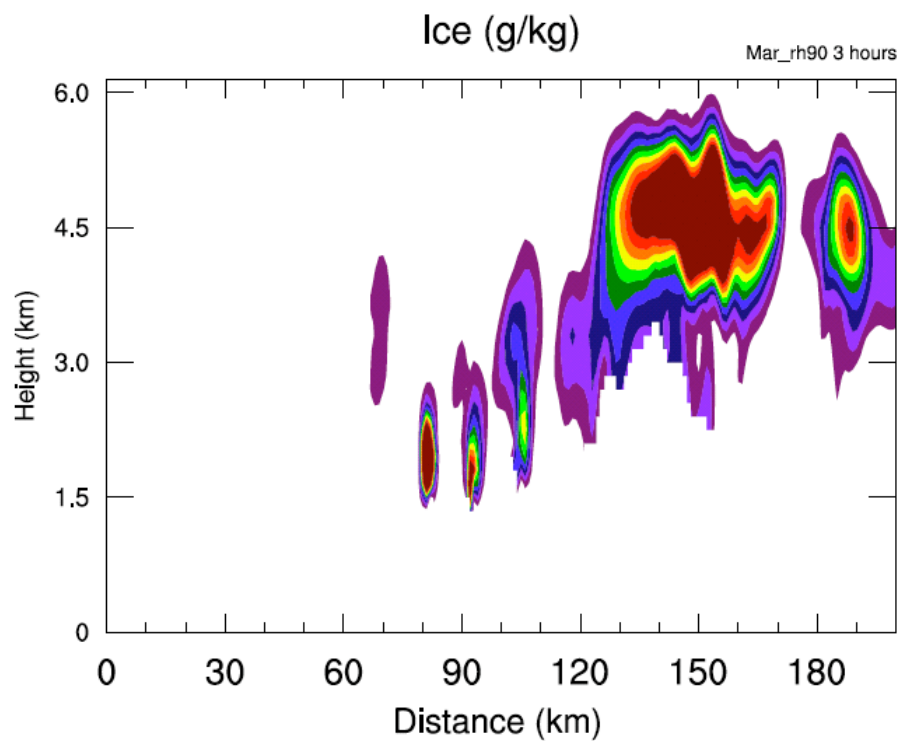
Figure 9: West to east cross-sections of cloud graupel content simulated with MAR-Control (left) and Con-Control (right) at 3 hours.
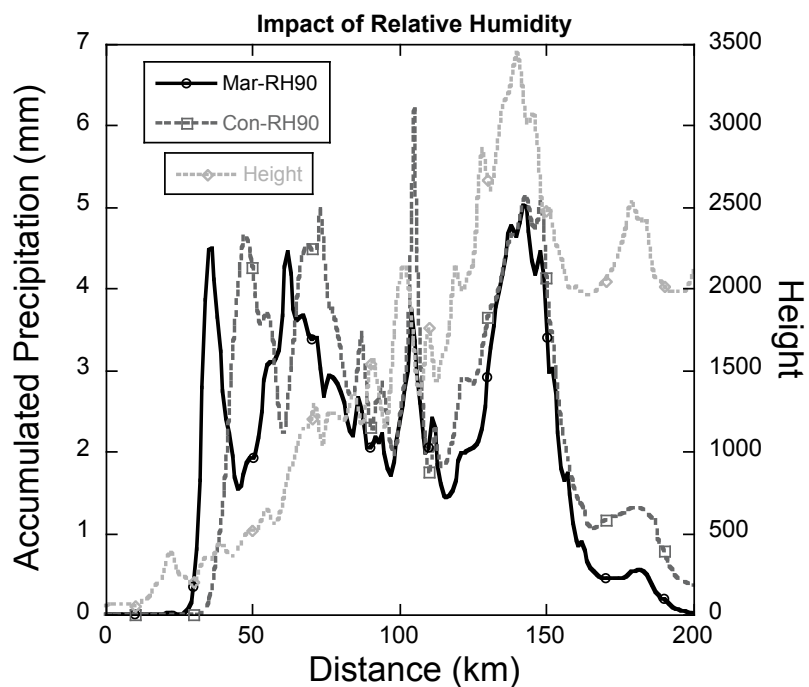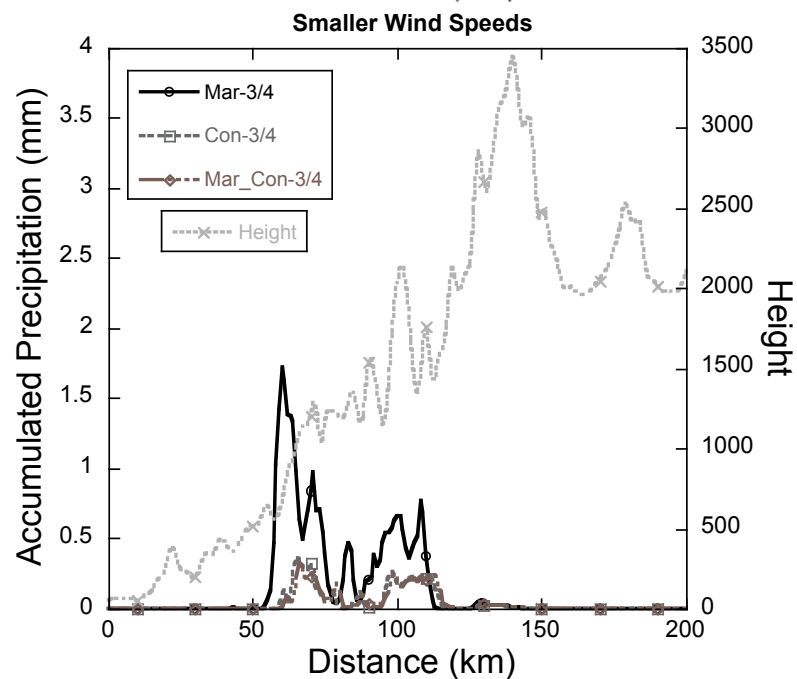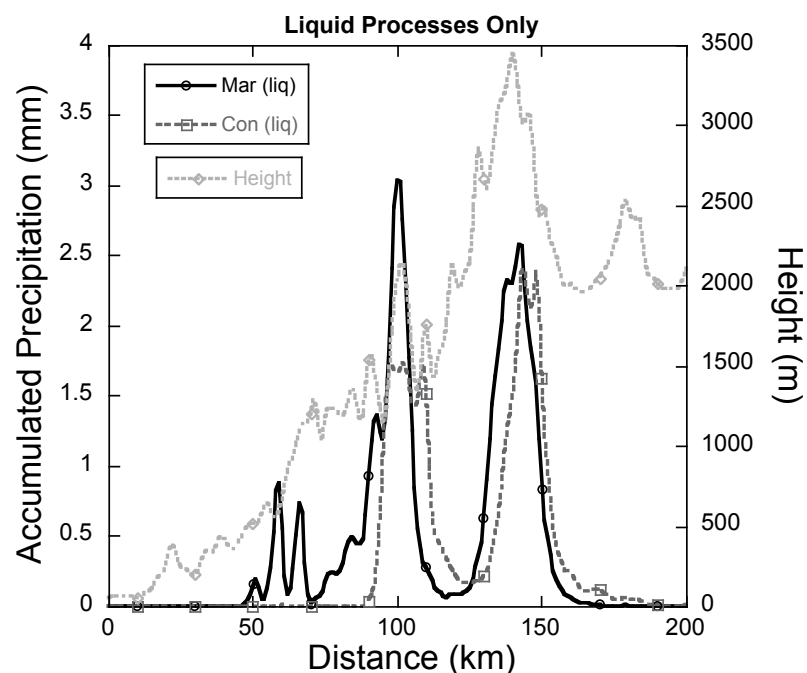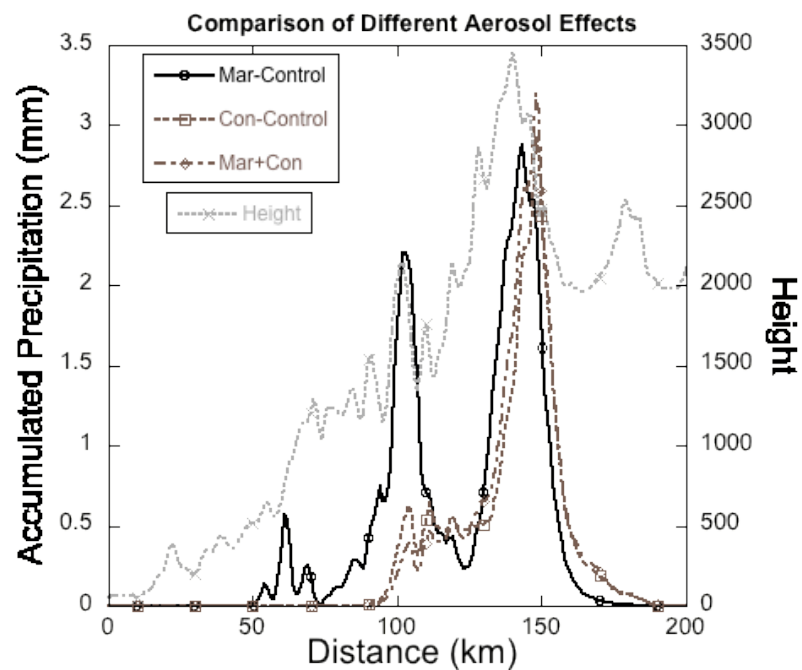
Figure 10: Accumulated Rainfall from simulations indicated in the label box.

Table 1: Accumulated precipitation (mm) obtained during 3 hours of simulation. The data were averaged over the mountain range (from the beginning of the mountain range to 200 km beyond).

- Model Run   Mar Con
- Control   0.44 0.32
- 3/4 Wind   0.16 0.04
- RH=90%   3.62 3.78
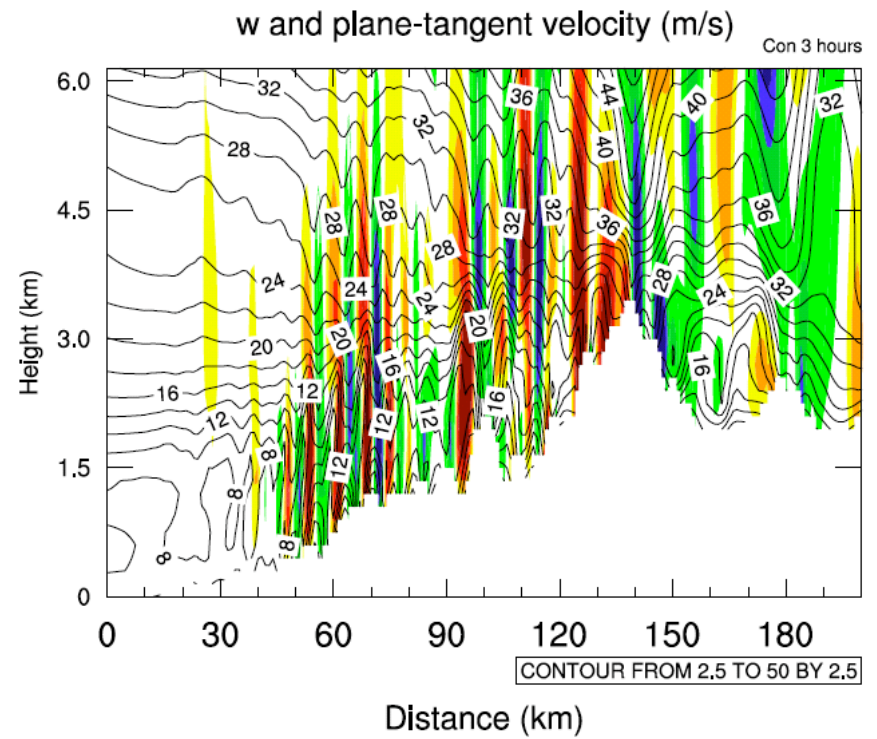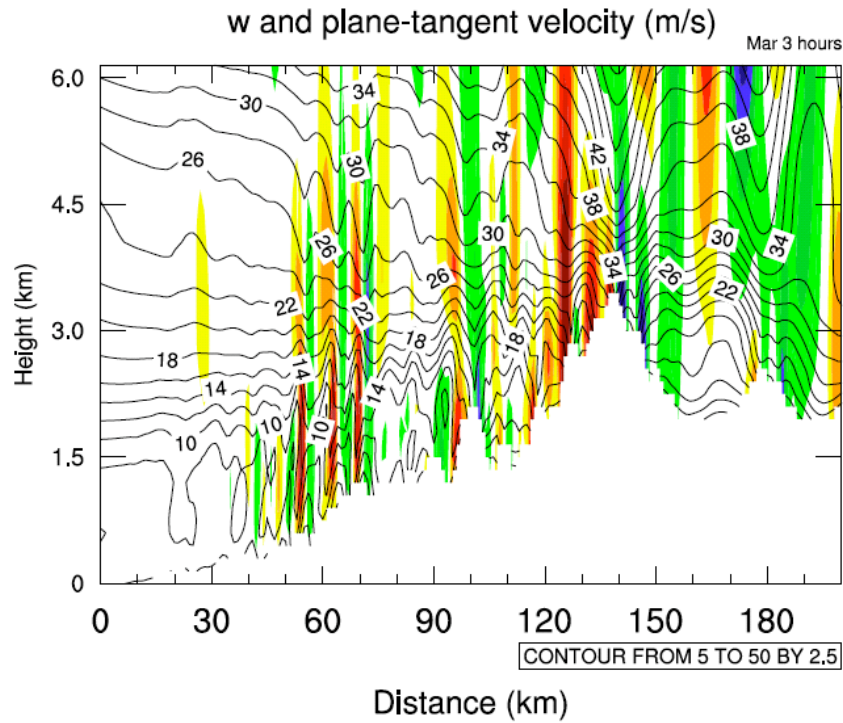
Figure 11: West to east cross-sections of vertical velocity simulated with MAR-Control (left) and Con-Control (right) at 3 hours.
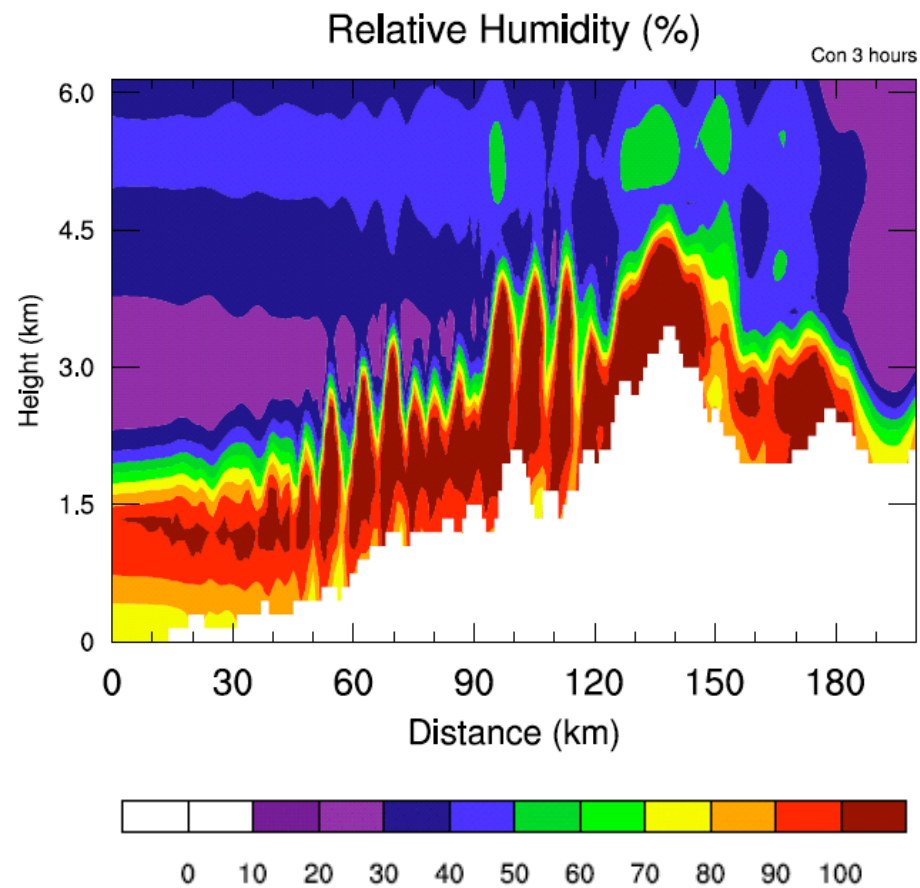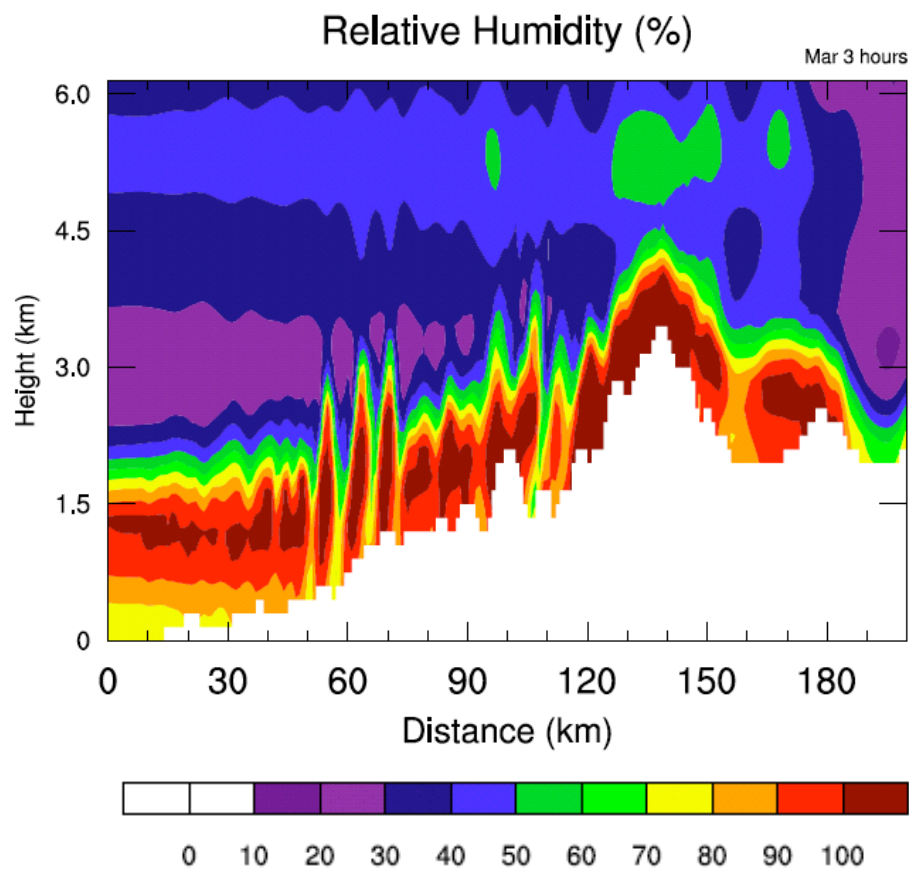
Figure 12: West to east cross-sections of relatively simulated with MAR-Control (left) and Con-Control (right) at 3 hours.
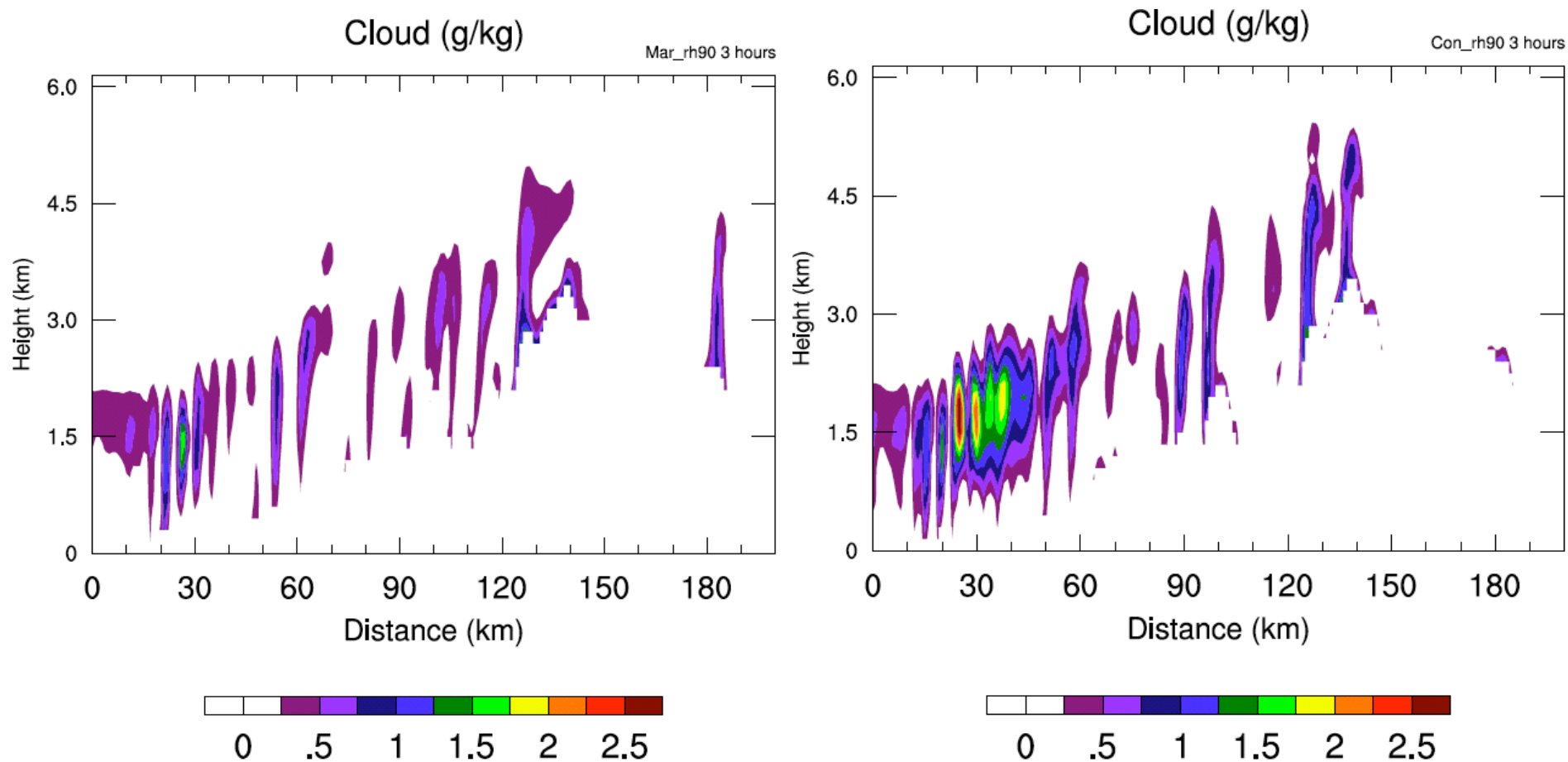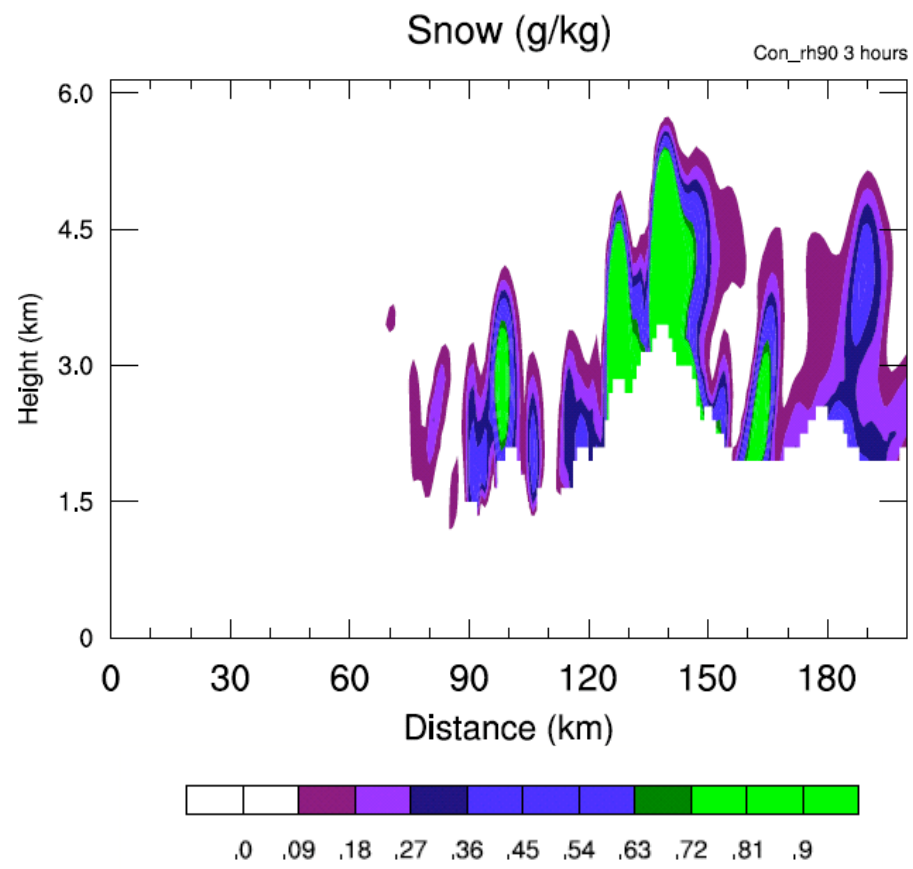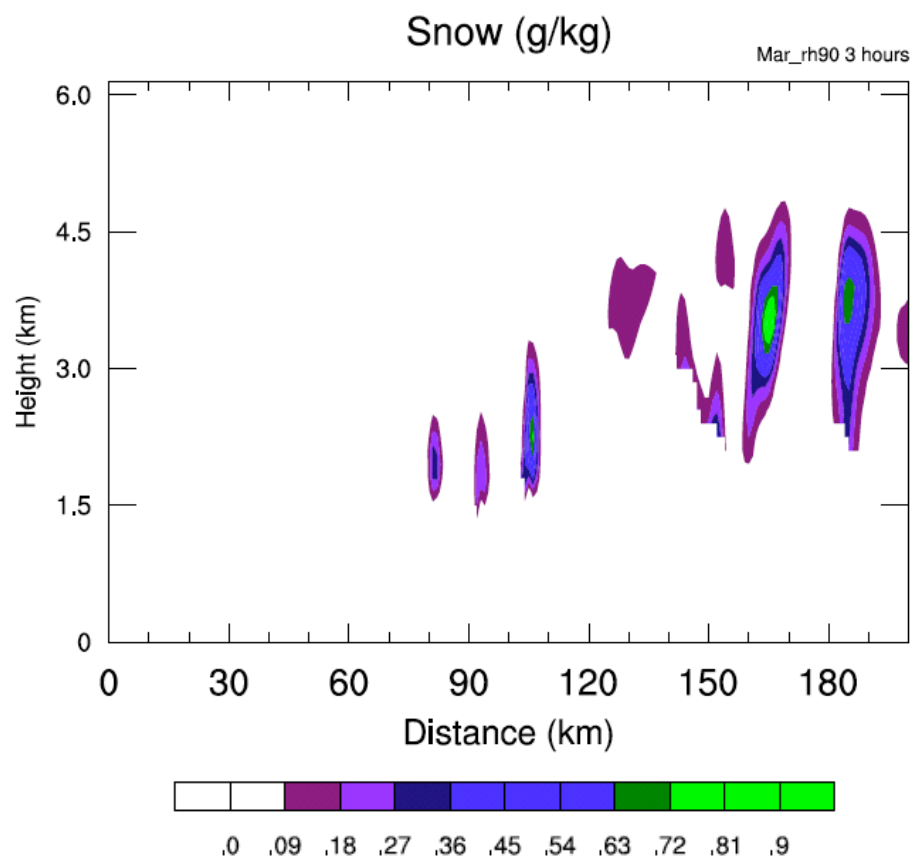
Figure 13: West to east cross-sections of cloud water content simulated with Mar-RH90 (left) and Con-RH90 (right) at 3 hours.
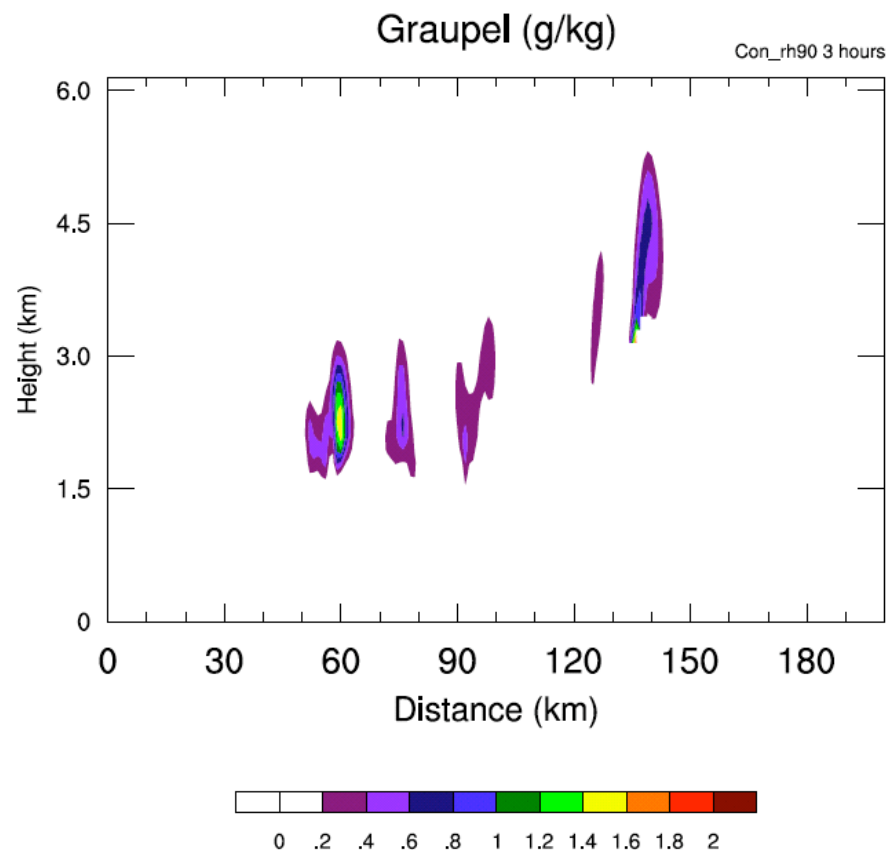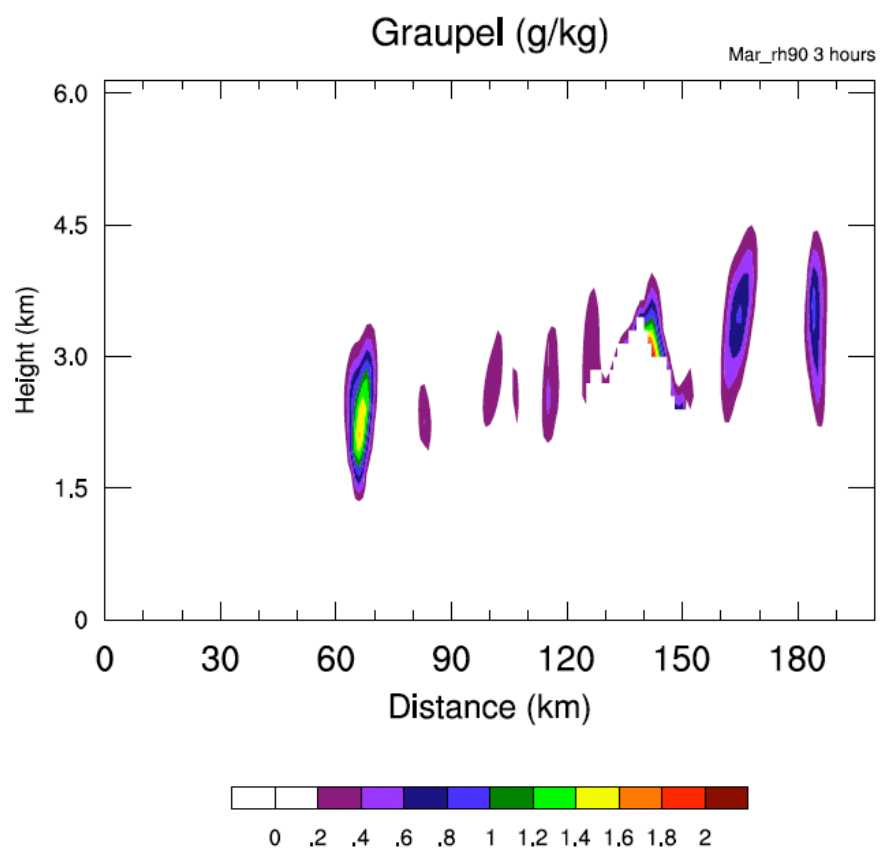
Figure 14: West to east cross-sections of cloud number concentration simulated with Mar-RH90 (left) and Con-RH90 (right) at 3 hours.

Figure 15: West to east cross-sections of cloud rain water content simulated with Mar-RH90 (left) and Con-RH90 (right) at 3 hours.

Figure 16: West to east cross-sections of cloud ice content simulated with Mar-RH90 (left) and Con-RH90 (right) at 3 hours.

Figure 17: West to east cross-sections of cloud snow content simulated with Mar-RH90 (left) and Con-RH90 (right) at 3 hours.

Figure 18: West to east cross-sections of cloud graupel content simulated with Mar-RH90 (left) and Con-RH90 (right) at 3 hours.
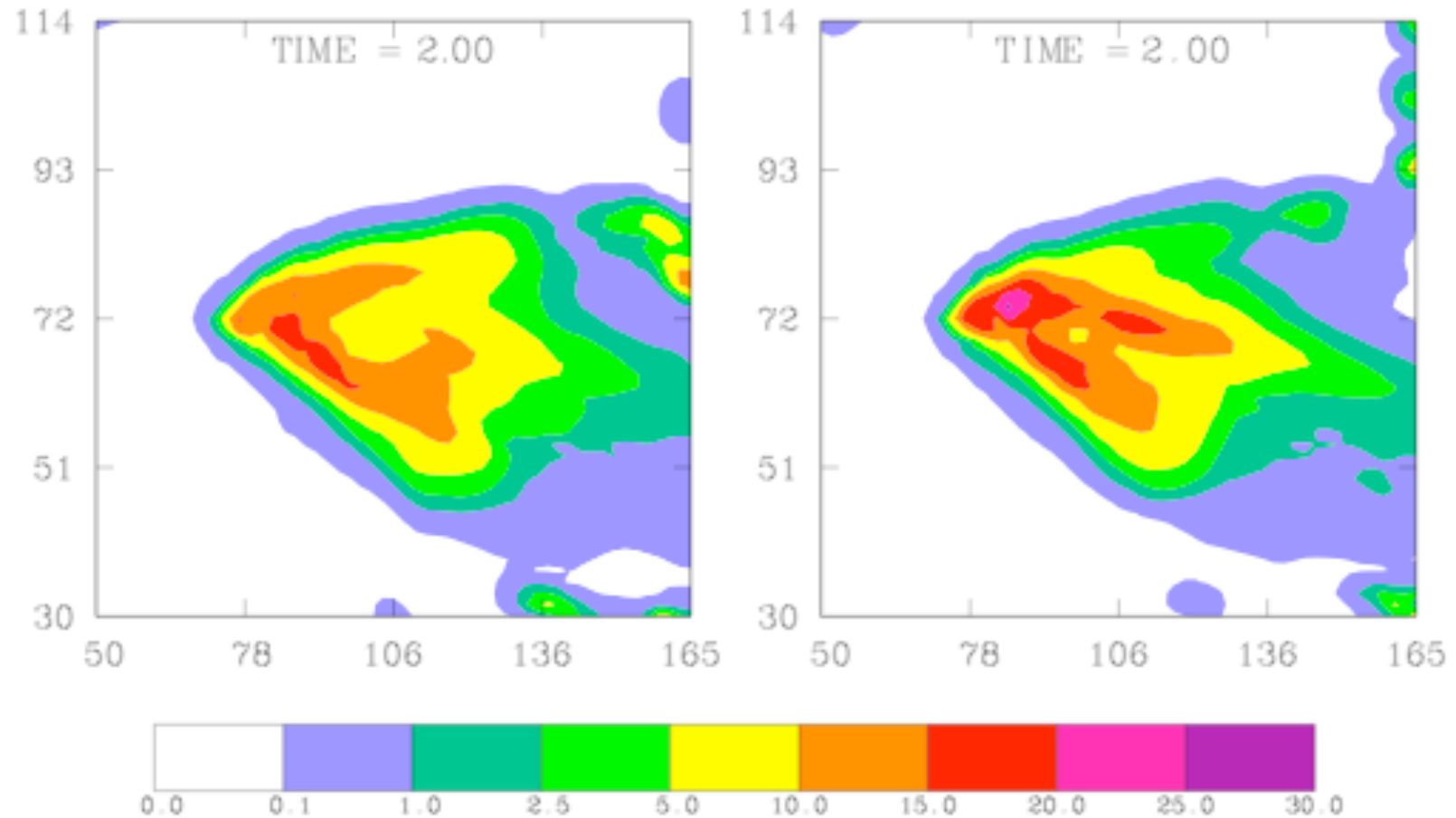
Super-Cell: High Humidity

Figure 19: Accumulated precipitation from super-cell simulations with maritime and continental aerosols..
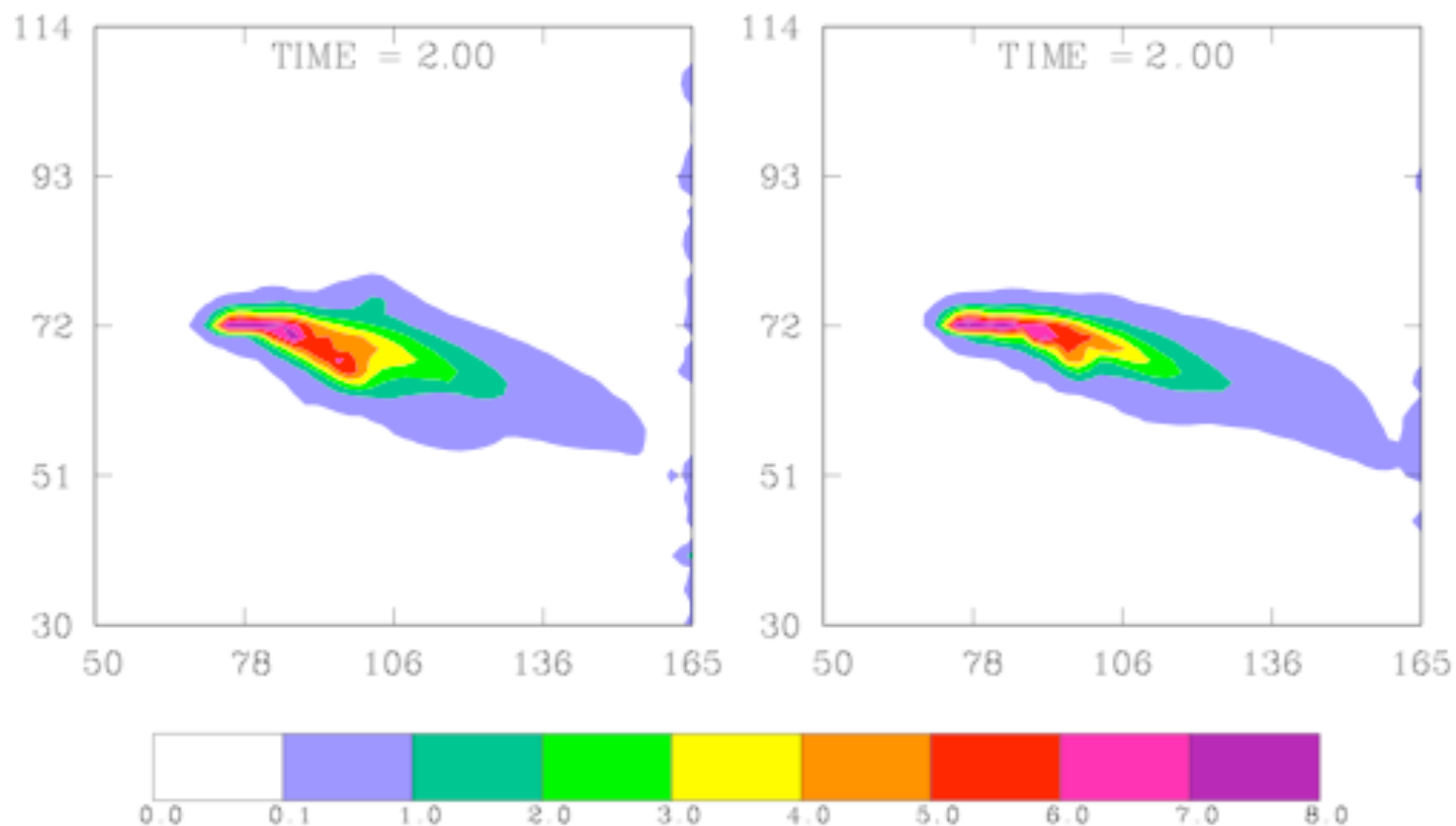
Super-Cell: Medium Humidity

Figure 20: Accumulated precipitation from super-cell simulations with maritime and continental aerosols at initial humidity no larger than 75%.
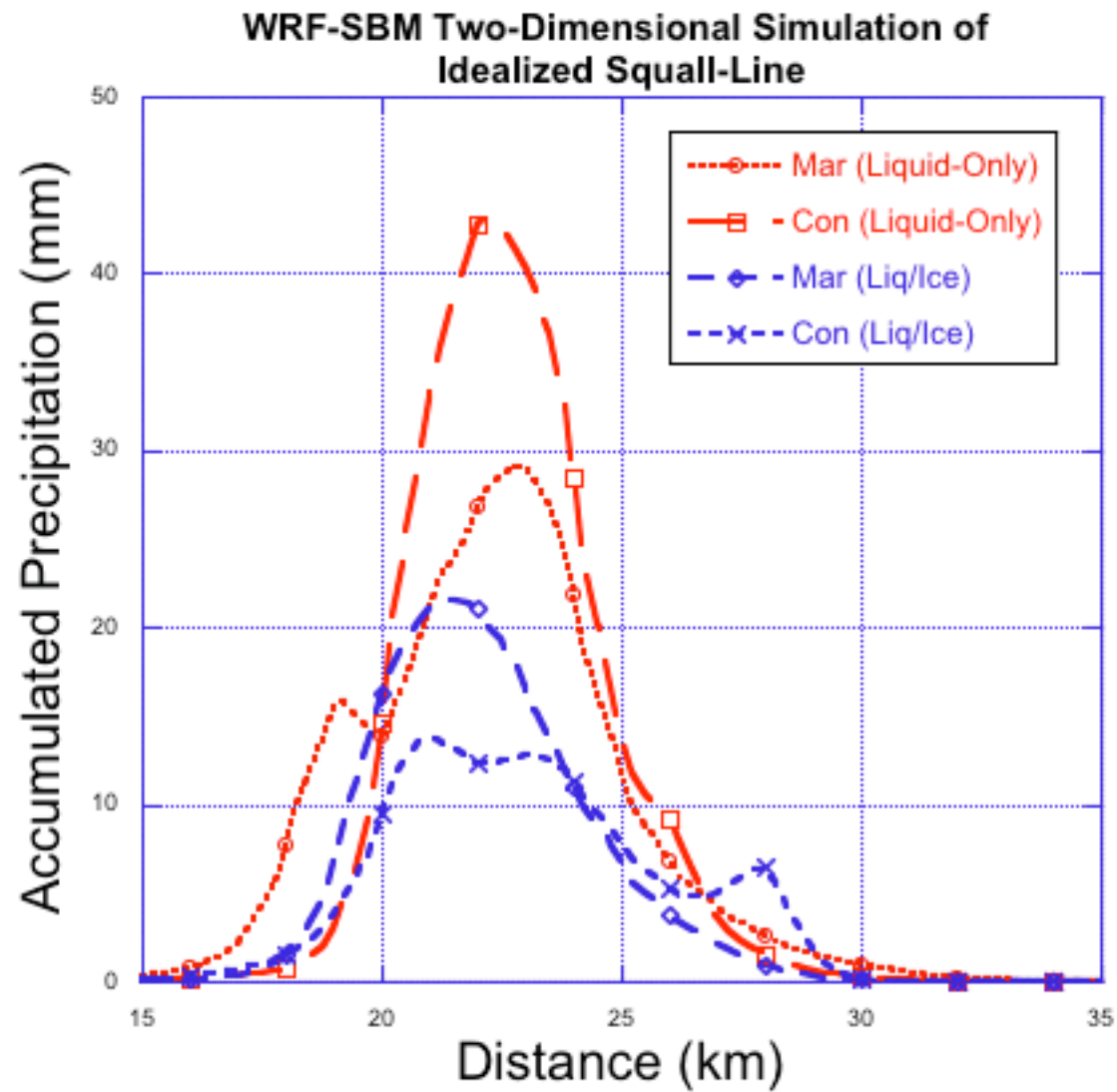
Figure 21: Accumulated precipitation from two-dimensional squall line simulations with maritime and continental aerosols for liquid only and mixed phase microphysical simulations.